Int. J. Solids Structures, 1973, Vol. 9, pp. 1237 to 1281. Pergamon Press. Printed in Great Britain

RECENT RESULTS IN NONLINEAR VISCOELASTIC WAVE PROPAGATION

KARL W. SCHULER and JACE W. NUNZIATO

Sandia Laboratories, Albuquerque, New Mexico 87115, U.S.A.

and

EDWARD K. WALSH

University of Florida, Gainesville, Florida 32601, U.S.A.

Abstract—In this article we present a review of some recent theoretical and experimental developments in the field of nonlinear viscoelastic wave propagation. Confining our attention to the case of one-dimensional strain, we review the theories of shock and acceleration wave propagation in general materials with memory and discuss the correlation of these theoretical predictions with some recent experimental results obtained for a particular polymeric solid. Fundamental to this work is the existence of steady shock waves and the fact that they can be generated in a one-dimensional experimental configuration. Using such experimental steady wave observations, a procedure is outlined for determining the material response functions necessary for predicting the growth or decay of shock and acceleration waves in viscoelastic materials. It is further shown that by using a particular constitutive assumption (either purely mechanical or thermomechanical) the complete one-dimensional constitutive equation governing the material response can be evaluated from steady shock wave measurements.

1. INTRODUCTION

DURING the past decade there has been considerable theoretical research in the field of continuum mechanics devoted to the study of the dynamic response of nonlinear viscoelastic materials. Many of these studies have dealt, in particular, with various aspects of one-dimensional wave propagation within the context of the general constitutive theory of materials with fading memory. These studies have considered the propagation of both shock and acceleration waves and have derived the conditions governing their growth and decay. These conditions imply the existence of steady waves in such dissipative media and proofs of their existence have been established.

During this same period, experimental developments in the field of shock wave physics have made it possible to produce high-amplitude plane waves by using a plate-impact configuration. In addition, instrumentation techniques based on laser interferometry have been developed which allow the fine structure of the wave to be observed with nanosecond resolution and high accuracy. Due to the inertial confinement in such experiments, extremely large one-dimensional strains are readily produced which generally result in nonlinear behavior of the material sample. In several recent studies, these experimental techniques have been employed to investigate one-dimensional wave propagation in a

particular viscoelastic material (polymethyl methacrylate) in an effort to show the correlation between experimental observations and the predictions of the general nonlinear theory of materials with memory. An important aspect of these studies is concerned with the propagation of steady shock waves. Using the experimental observations of steady shock wave profiles and the corresponding theoretical results, it was found that a complete one-dimensional constitutive equation (either mechanical or thermomechanical) could be determined for the material. This constitutive model then serves to determine the material response functions necessary to predict the growth and decay behavior of shock and acceleration waves. These predictions have been found to be in very good agreement with experimental results.

In this article, we collect the main results of this work and give a unified presentation of one-dimensional wave propagation in nonlinear viscoelastic materials. There is no attempt to cover completely all the research carried out in the last ten years in viscoelastic wave propagation; rather we concentrate on that portion of the field directly related to the geometrical configuration of one-dimensional strain. Further, our emphasis is placed on the physical aspects of the theory, the methods for determining the relevant material functions from experimental data, and the correlation between theory and experiment. It should be noted that while all the experimental data presented concerns the solid polymer, polymethyl methacrylate (PMMA), we expect the theory and methods discussed will be applicable to other polymeric materials.

Following a brief discussion in Section 2 of the kinematics of one-dimensional motions and the classification of waves, we review the general mechanical theories of shock and acceleration wave propagation in nonlinear materials with fading memory. The steady wave problem and the results of studies on the existence of steady wave solutions in nonlinear dissipative media are also discussed. In Section 4 the experimental techniques used to study the evolutionary behavior of shock and acceleration waves are described in detail.

The next three sections deal with various aspects of shock and acceleration wave propagation and the comparison of theory and experiment. In Section 5 the analysis of the steady shock wave problem assuming a mechanical constitutive model is considered in detail including the determination of material functions and the steady wave solutions. Then, in Section 6, using the constitutive model and material response functions obtained in the steady wave study, two problems associated with shock wave growth and decay are considered. The first involves the determination of the *critical acceleration* which has been shown to govern the growth or decay behavior of a propagating shock front and the second deals with the attenuation of thin shock pulses. In Section 7, we discuss acceleration wave speeds and the use of the model and the response functions to predict the behavior of acceleration waves. In this case, the growth or decay of the wave is governed by a *critical amplitude*.

In Section 8, we discuss the role of thermodynamics in one-dimensional viscoelastic wave propagation. After a brief review of recent results of the thermodynamics of materials with memory, the steady shock wave problem and the determination of material response functions for a thermoviscoelastic constitutive model is considered. Then consideration is given to the growth and decay of shock waves including thermodynamic influences. Finally, the use of the constitutive model in predicting stress–energy response is discussed. Again, in each case, the comparison of experimental results with theoretical predictions is presented.

2. KINEMATICS OF ONE-DIMENSIONAL MOTIONS

2.1 *Kinematics and balance laws*

Throughout this discussion, we shall confine our attention to one-dimensional motions in homogeneous viscoelastic solids. The motion of a material is described by the continuous function $u = u(X, t)$ giving the displacement u at time t of the material particle which occupied the position X in a fixed reference configuration with density ρ_R. Thus, it is convenient to identify the body in its reference configuration with an interval of the real line R and each material point with its position X in R. Assuming suitable smoothness of the motion, we define

$$v = \partial_t u(X, t), \quad \varepsilon = -\partial_X u(X, t) \tag{2.1}$$

as the particle velocity and strain, respectively. In addition, we consider the one-dimensional stress σ, absolute temperature $\theta > 0$, internal energy e (in units of energy per unit volume), entropy η, and free energy $\psi = \mathrm{e} - \theta\eta$ to also be functions of X and t. Since all the experimental data to be presented has been obtained for compressive loading, it is convenient to take stress and strain positive in compression. While this is the convention usually followed in the shock wave physics literature, it is not the convention generally followed in the mechanics literature.

In one dimension, mass balance requires that the present density $\rho(X, t)$ be related to the reference density ρ_R by

$$\rho(X, t) = \frac{\rho_R}{1 - \varepsilon(X, t)}. \tag{2.2}$$

Since $\rho > 0$, we necessarily have $-\infty < \varepsilon < 1$. Neglecting heat conduction, external body forces and external heat supplies, the balance of linear momentum and energy take the form

$$\frac{\mathrm{d}}{\mathrm{d}t}\int_{X_1}^{X_2} \rho_R v(X, t)\,\mathrm{d}X = \sigma(X_1, t) - \sigma(X_2, t), \tag{2.3}$$

$$\frac{\mathrm{d}}{\mathrm{d}t}\int_{X_1}^{X_2} [\tfrac{1}{2}\rho_R v^2(X, t) + \mathrm{e}(X, t)]\,\mathrm{d}X = \sigma(X_1, t)v(X_1, t) - \sigma(X_2, t)v(X_2, t), \tag{2.4}$$

respectively; and the second law of thermodynamics (Clausius–Duhem inequality) asserts that

$$\frac{\mathrm{d}}{\mathrm{d}t}\int_{X_1}^{X_2} \rho_R \eta(X, t)\,\mathrm{d}X \geq 0. \tag{2.5}$$

The equations (2.3)–(2.5) hold for all times t and for every interval $[X_1, X_2]$ in R.

2.2 *Classification of waves*

By a *wave*, we mean a motion which contains a propagating disturbance. Here we shall be particularly interested in waves involving jump discontinuities in certain kinematical and thermal fields.† The *intrinsic velocity* U of such a discontinuity (wave front)

† Multiple waves may involve multiple discontinuities, e.g. Sections 4 and 7.1.

is defined by

$$U(t) = \frac{\mathrm{d}Y(t)}{\mathrm{d}t} \tag{2.6}$$

where $Y(t)$ is the material point in R at which the front is to be found at time t. Thus, the intrinsic velocity expresses the rate of advance of the front with respect to the material in the reference configuration and $Y(t)$, $t > 0$, gives the trajectory of the front. Here we use the standard notation for the jump $[f]$ in a function $f(X, t)$ across the wave front; i.e.†

$$[f](t) = f^-(t) - f^+(t), \quad f^\pm(t) = \lim_{X \to Y^\pm(t)} f(X, t). \tag{2.7}$$

With $U > 0$, f^+ and f^- are the limiting values of $f(X, t)$ immediately ahead of and behind the wave front. If $\dot{f}(X, t) = \partial_t f(X, t)$ and $\partial_X f(X, t)$ are also discontinuous at $X = Y(t)$ but continuous everywhere else, then

$$\frac{\mathrm{d}[f]}{\mathrm{d}t} = [\dot{f}] + U[\partial_X f]. \tag{2.8}$$

This kinematical condition of compatibility is given in a more general context by Truesdell and Toupin [1].‡

We assume throughout this article that the displacement $u(X, t)$ is a continuous function of X, t for all X, t. A *shock wave* is a motion containing a wave front across which the strain ε, the particle velocity v, the temperature θ and their derivatives are discontinuous. Thus, (2.8) with $f = u$ asserts that at $X = Y(t)$

$$[v] = U[\varepsilon]. \tag{2.9}$$

It is clear from (2.9) that either $[v]$ or $[\varepsilon]$ can be taken as a measure of the *amplitude* of the shock. The stress and the internal energy are also, in general, discontinuous at $X = Y(t)$ and the balance laws (2.3) and (2.4) imply that§

$$[\sigma] = \rho_R U[v], \quad [\partial_X \sigma] = -\rho_R[\dot{v}], \tag{2.10}$$

$$-U[\mathrm{e} + \tfrac{1}{2}\rho_R v^2] = [\sigma v], \quad [\dot{\mathrm{e}}] = [\sigma\dot{\varepsilon}]. \tag{2.11}$$

The second law requires that‖

$$[\eta] \geq 0. \tag{2.12}$$

An *acceleration wave* is a one-dimensional motion containing a wave front across which the strain ε, the particle velocity v, and the temperature θ are continuous, but their derivatives are not. Thus, (2.8) with $f = v$ and $f = \varepsilon$ asserts that at $X = Y(t)$

$$[\dot{v}] = U[\dot{\varepsilon}] = U^2[\partial_X \varepsilon]. \tag{2.13}$$

The jump in the particle acceleration is taken as the *amplitude* $a(t)$ of the wave front:

$$a(t) = [\dot{v}]. \tag{2.14}$$

The balance relations (2.10) and (2.11) also hold for an acceleration wave.

† Cf. Truesdell and Toupin [1], Section 173.
‡ See also Coleman and Gurtin [2].
§ Cf. Truesdell and Toupin [1], Sections 205 and 241.
‖ Cf. Truesdell and Toupin [1], Section 258.

In a *smooth structured wave*, all kinematical and thermal fields are continuous and have continuous derivatives.

3. WAVES IN MATERIALS WITH MEMORY

Here we consider the propagation and growth of one-dimensional waves in nonlinear materials with long-range viscoelastic memory. For the time being, thermodynamic influences will be neglected and we omit giving the proofs of the main results. Thermodynamic effects in wave propagation will be considered in Section 8.

3.1. *Constitutive assumption*

The purely mechanical, one-dimensional response of a nonlinear material with memory can be characterized by the following general constitutive assumption:

(i) at a given material particle the stress at time t is determined by the entire history of the strain ε^t; i.e.

$$\sigma(t) = \mathscr{S}(\varepsilon^t) \tag{3.1}$$

where $\varepsilon^t(s) = \varepsilon(t-s)$, $0 \leq s < \infty$; and

(ii) the material exhibits "fading memory".

The concept of fading memory has been made mathematically precise by Coleman and Noll [3, 4] and implies that the stress functional $\mathscr{S}$ has certain smoothness properties. Let

$$\|\varepsilon^t\| = \left\{|\varepsilon(t)|^2 + \int_0^\infty h^2(s)|\varepsilon^t(s)|^2 \, ds\right\}^{\frac{1}{2}} \tag{3.2}$$

denote the norm of the history ε^t where $h(s)$ is a fixed influence function; i.e. a continuous, monotone-decreasing, square-integrable function. The set of all histories with finite norm forms a Hilbert space. Then, the constitutive functional $\mathscr{S}$ is assumed to be defined on this space and to be twice continuously differentiable; i.e. the derivatives $\partial_\varepsilon \mathscr{S}(\varepsilon^t)$ and $\partial_\varepsilon^2 \mathscr{S}(\varepsilon^t)$ exist, where the partial differentiation is with respect to the present value $\varepsilon = \varepsilon^t(0)$. Since $h(s)$ is monotone decreasing, the material response is influenced more by changes in the deformation in the recent past (small s) than by those occurring in the distant past (large s).

Using the assumed smoothness of the functional $\mathscr{S}$, Coleman and Noll [4] have shown that (3.1) can be approximated by†

$$\mathscr{S}(\varepsilon^t + \gamma^t) = \mathscr{S}(\varepsilon^t) + G_t(0)\gamma^t(0) + \int_0^\infty G_t'(s)\gamma^t(s)\, ds + o(\|\gamma^t\|) \tag{3.3}$$

as $\|\gamma^t\| \to 0$. Thus, for small relative strain histories γ^t, the response of a nonlinear material with memory is approximated by the constitutive equation of linear viscoelasticity. In equation (3.3), $G_t(s)$ is the *stress relaxation function* corresponding to the underlying strain history ε^t and $G_t'(s) = dG_t(s)/ds$. When it seems appropriate to emphasize the dependence

† See also Coleman, Gurtin and Herrera [5].

of $G_t(s)$ on the history ε^t we retain the functional notation and write $G_t(s) = \mathcal{G}(\varepsilon^t; s)$. Hereafter we assume that the $\lim_{s\to\infty} \mathcal{G}(\cdot; s) = \mathcal{G}(\cdot; \infty)$ exists and it is not difficult to show that $\mathcal{G}(\varepsilon^t; 0) = \partial_\varepsilon \mathcal{S}(\varepsilon^t)$.

Now consider the special strain history

$$\varepsilon_I(s) = \begin{cases} \varepsilon, & s = 0 \\ 0, & s > 0 \end{cases} \tag{3.4}$$

corresponding to a strain jump ε suddenly applied to a material point which has been unstrained for all past time. The stress $\sigma = \mathcal{S}(\varepsilon_I)$ depends only on the strain jump ε and thus we call

$$\sigma_I(\varepsilon) = \mathcal{S}(\varepsilon_I)$$

the *instantaneous response function*. The function σ_I is of class C^2 and the derivatives

$$E_I = \frac{d\sigma_I(\varepsilon)}{d\varepsilon}, \qquad \tilde{E}_I = \frac{d^2\sigma_I(\varepsilon)}{d\varepsilon^2}, \tag{3.5}$$

are called the *instantaneous tangent modulus* and the *instantaneous second-order modulus*, respectively. The stress relaxation function corresponding to the underlying strain history (3.4) is designated as $G(\varepsilon; s) \equiv \mathcal{G}(\varepsilon_I; s)$ and

$$E_I(\varepsilon) = G(\varepsilon; 0). \tag{3.6}$$

It shall also prove useful to define the *equilibrium response function* for the material:

$$\sigma_E(\varepsilon) = \mathcal{S}(\varepsilon_E)$$

which gives the stress corresponding to the equilibrium (constant) strain history $\varepsilon_E(s) = \varepsilon$, $0 \le s < \infty$. The function σ_E is also of class C^2 and the *equilibrium tangent modulus* and *equilibrium second-order modulus* are given by

$$E_E = \frac{d\sigma_E(\varepsilon)}{d\varepsilon}, \qquad \tilde{E}_E = \frac{d^2\sigma_E(\varepsilon)}{d\varepsilon^2}. \tag{3.7}$$

For our discussion of wave propagation, it is appropriate to impose certain curvature conditions on the stress functional $\mathcal{S}$ which are expected to hold for most viscoelastic materials. In particular, it will be assumed that for all ε on (0, 1) and all s on $[0, \infty)$

$$\begin{aligned} &\sigma_I(\varepsilon) > \sigma_E(\varepsilon) > 0, \\ &E_I(\varepsilon) > E_E(\varepsilon) > 0, \\ &\tilde{E}_I(\varepsilon) > 0, \qquad \tilde{E}_E(\varepsilon) > 0, \end{aligned} \tag{3.8}$$

and

$$\mathcal{G}(\varepsilon^t; s) > 0, \qquad \mathcal{G}^r(\varepsilon^t; s) \le 0. \tag{3.9}$$

The inequalities (3.8) imply that the instantaneous and equilibrium stress–strain curves are strictly convex from below and that the instantaneous curve lies everywhere above the equilibrium curve (cf. Fig. 1). We also assume that $\sigma_I(0) = \sigma_E(0) = 0$. The inequalities (3.9) assert that for all strain histories on (0, 1) the stress relaxation function is positive and a monotone decreasing function of the elapsed time s. Bowen and Chen [6] have recently

shown that the inequality $(3.9)_2$, evaluated for $\varepsilon^t(s) = \varepsilon_E(s)$ and $s = 0$, follows as a consequence of the second law. The relation of this inequality to internal dissipation has also been discussed by Gurtin and Herrera [7] in the context of linear viscoelasticity.

3.2 *Acceleration waves*

The propagation of acceleration waves in materials with memory has been considered in detail by Coleman, Gurtin and Herrera [2, 5]. They showed that the intrinsic velocity U of an acceleration wave propagating into a region with an arbitrary strain history ε^t satisfies

$$U^2(t) = \frac{\partial_\varepsilon \mathscr{S}(\varepsilon^t)}{\rho_R}. \tag{3.10}$$

Coleman and Gurtin [2] also showed that if the acceleration wave amplitude $a(t)$ is given at $t = 0$, then it is possible to derive an expression for $a(t)$ at later times, the form of the expression depending upon the strain history of the region traversed by the wave front up to time t. For simplicity, we give their results only for waves propagating into unstrained regions in equilibrium, i.e. for $X > Y(t), \varepsilon^t(s) = 0, 0 \leq s < \infty$. In this case, we let

$$(E_I)_0 = \left.\frac{\mathrm{d}\sigma_I(\varepsilon)}{\mathrm{d}\varepsilon}\right|_{\varepsilon=0}, \qquad (\tilde{E}_I)_0 = \left.\frac{\mathrm{d}^2\sigma_I(\varepsilon)}{\mathrm{d}\varepsilon^2}\right|_{\varepsilon=0}, \qquad G_0'(0) = \mathscr{G}'(0;0), \tag{3.11}$$

and note that the intrinsic velocity $U = U_0$ is a constant given by $\rho_R U_0^2 = (E_I)_0$. It follows that, under these conditions, the acceleration wave amplitude $a(t)$ satisfies the equation

$$\frac{\mathrm{d}a}{\mathrm{d}t} = -\beta a + \frac{\beta}{a_c} a^2 \tag{3.12}$$

where β and a_c are constants given by

$$\beta = -\frac{G_0'(0)}{2(E_I)_0}, \qquad a_c = -\frac{G_0'(0)U_0}{(\tilde{E}_I)_0}. \tag{3.13}$$

This differential equation is a Bernoulli equation† with the solution‡

$$a(t) = \frac{a_c}{\left(\dfrac{a_c}{a(0)} - 1\right)\exp(\beta t) + 1}. \tag{3.14}$$

Thus, in the case of an acceleration wave, an exact closed-form expression for the time-dependent behavior of the jump in particle acceleration can be obtained which depends only on the properties of the material.

From the curvature assumptions given in Section 3.1, it follows that $\beta > 0$ and $a_c > 0$. Thus, for a compressive wave with $a(0) > 0$ it follows from (3.14) that§

† The general properties of the Bernoulli equation (3.12) with time dependent coefficients have been studied by Bailey and Chen [8].

‡ A similar result was obtained by Varley [9] for materials in which the stress functional $\mathscr{S}$ is represented by a multi-integral expansion. Coleman, Greenberg and Gurtin [10] have also obtained this result for another class of viscoelastic materials (called Maxwellian materials) which in general may not be completely included in the constitutive assumption (i) and (ii). Maxwellian materials obey the constitutive law $\dot{\sigma} = E(\varepsilon, \sigma)\dot{\varepsilon} + G(\varepsilon, \sigma)$; cf. Noll [11].

§ Cf. Coleman and Gurtin [2], Theorem 4.2.

(i) if $a(0) < a_c$, $a(t) \to 0$ as $t \to \infty$,
(ii) if $a(0) = a_c$, $a(t) \equiv a(0)$, or
(iii) if $a(0) > a_c$, $a(t) \to \infty$ monotonically in a finite time t_∞,

$$t_\infty = -\frac{1}{\beta} \ln\left(1 - \frac{a_c}{a(0)}\right). \tag{3.15}$$

Clearly, a_c plays the role of a *critical amplitude*. If the amplitude is less than the critical amplitude, then the internal dissipation of the material (manifested by a strictly negative value of $G_0'(0)$) is the governing effect and the wave front decays. However, if the amplitude is greater than the critical value, then the nonlinearity of the instantaneous stress–strain curve is the dominating effect and the acceleration wave front achieves an infinite amplitude in a finite time. It has been conjectured that the approach of $a(t)$ to ∞ as $t \to t_\infty$ is indicative of the formation of a shock wave at time t_∞. In Section 7.2, we shall discuss some experimental results reported by Walsh and Schuler [12] which support this conjecture.

3.3 *Shock waves*

The general theory of the propagation of one-dimensional shock waves in nonlinear materials with fading memory characterized by (3.1) has been developed by Coleman, Gurtin and Herrera [5] and by Chen and Gurtin [13]. In particular, Chen and Gurtin showed that the growth and decay behavior of a shock discontinuity is governed by a differential equation relating the strain ε^- to the strain gradient $(\partial_X \varepsilon)^-$ behind the front.† Following their analysis, we consider a *compressive wave* propagating into a region at rest and unstrained for all past times, i.e. for $X > Y(t), \varepsilon^t(s) = 0$ on $0 \leq s < \infty$ and

$$[\![\varepsilon]\!] = \varepsilon^- > 0, \qquad [\![\partial_X \varepsilon]\!] = (\partial_X \varepsilon)^-. \tag{3.16}$$

It follows from the definition of the instantaneous response function σ_I that $[\![\sigma]\!] = \sigma_I(\varepsilon^-)$. Thus (2.9) and (2.10) imply that the intrinsic velocity U is given by‡

$$\rho_R U^2 = \frac{\sigma_I(\varepsilon^-)}{\varepsilon^-} \tag{3.17}$$

and by the convexity condition $(3.8)_3$

$$\frac{\rho_R U^2}{E_I^-} \equiv \hat{\mu} < 1 \tag{3.18}$$

where $E_I^- = E_I(\varepsilon^-)$. The inequality (3.18) asserts that the shock velocity is always subsonic with respect to the material behind the wave front. Clearly by (3.17) the shock velocity depends on the strain amplitude ε^- and in fact

$$\frac{dU}{dt} = \frac{(1-\hat{\mu})E_I^-}{2\rho_R U \varepsilon^-} \frac{d\varepsilon^-}{dt}. \tag{3.19}$$

† See also Huilgol [14]. Lubliner and Secor [15] have derived a similar relation for viscoelastic materials with the stress functional represented by a multi-integral expansion. Duvall and Alverson [16] and Ahrens and Duvall [17] have also derived such a relation for Maxwellian materials.

‡ Cf. Coleman, Gurtin and Herrera [5].

Thus, the shock velocity increases, decreases, or remains the same according to whether the shock amplitude ε^- increases, decreases, or remains the same.

Using the properties of shock waves and the assumed smoothness of the stress function $\mathscr{S}$, Chen and Gurtin [13] derived the *shock amplitude equation*

$$\frac{d\varepsilon^-}{dt} = U\frac{(1-\hat{\mu})}{(1+3\hat{\mu})}\{\hat{\lambda}-(\partial_X\varepsilon)^-\} \tag{3.20}$$

where

$$\hat{\lambda} = \frac{G'(\dot{\varepsilon}^-;0)\varepsilon^-}{UE_I^-(1-\hat{\mu})}. \tag{3.21}$$

Here $G'(\varepsilon^-;0)$ is the initial slope of the stress relaxation function corresponding to the jump strain history (3.4); thus, by the curvature assumption $(3.9)_2$, $\hat{\lambda} \leq 0$. It is immediately evident from (3.18) and the amplitude equation (3.20) that the growth or decay behavior of the wave front depends on the strain gradient immediately behind the front; i.e.

(i) if $\hat{\lambda} < (\partial_X\varepsilon)^-$, $\quad \dfrac{d\varepsilon^-}{dt} < 0$,

(ii) if $\hat{\lambda} = (\partial_X\varepsilon)^-$, $\quad \dfrac{d\varepsilon^-}{dt} = 0$, or

(iii) if $\hat{\lambda} > (\partial_X\varepsilon)^-$, $\quad \dfrac{d\varepsilon^-}{dt} > 0$.

In view of the steady wave condition (ii), $\hat{\lambda}$ is called the *critical strain gradient.*

Experimental shock wave studies involve the measurement of particle velocity histories at given material points in a sample, and thus it is often more convenient to express the amplitude equation (3.20) in terms of particle velocity:

$$\frac{dv^-}{dt} = \frac{(1-\hat{\mu}^2)}{(1+3\hat{\mu})}\{(\dot{v})^- - U^2|\hat{\lambda}|\}. \tag{3.22}$$

Here $(\dot{v})^-$ is the particle acceleration immediately behind the shock front and $U^2|\hat{\lambda}|$ is the *critical acceleration.* Clearly, the front grows if $(\dot{v})^- > U^2|\hat{\lambda}|$, decays if $(\dot{v})^- < U^2|\hat{\lambda}|$, or is steady if $(\dot{v})^- = U^2|\hat{\lambda}|$.

It should be noted that in general it is not possible to determine the particle velocity amplitude v^- of a shock wave as a function of time from the differential equation (3.22) because the particle acceleration $(\dot{v})^-$ is not known in advance. The value of this quantity at each instant reflects the initial and boundary conditions associated with the generation and subsequent propagation of the shock wave. However, there are certain shock wave problems in which approximate solutions of (3.22) can be obtained (we shall discuss one such problem in Section 6.2).

In the case of weak shock discontinuities, it can be shown that the shock amplitude equation (3.22) reduces to†

$$\frac{dv^-}{dt} = -\beta v^-$$

† Cf. Chen and Gurtin [13].

where β is the constant defined in $(3.13)_1$. This equation has the solution

$$v^-(t) = v^-(0)\exp(-\beta t)$$

which implies that the amplitude of a weak shock front decays exponentially to zero as $t \to \infty$.† It can also be shown that‡

$$\begin{aligned} \lim_{v^- \to 0} U &= U_0, \\ \lim_{v^- \to 0} U^2|\hat{\lambda}| &= 2a_c, \end{aligned} \tag{3.23}$$

where $\rho_R U_0^2 = (E_I)_0$ and a_c is given by $(3.13)_2$. Thus, as the amplitude of the shock discontinuity tends to zero, the intrinsic shock velocity is approximated by the intrinsic acceleration wave velocity U_0 and the critical acceleration has as its limit twice the critical amplitude a_c of an acceleration wave propagating into an unstrained equilibrium region.§

3.4 *Steady waves*

The results of the previous sections for shock and acceleration waves suggest the possible existence of steady waves in nonlinear materials with memory. The existence of such waves was first demonstrated by Pipkin [21]. Using the specific constitutive assumption of finite linear viscoelasticity formulated by Coleman and Noll [4], Pipkin obtained exact solutions to the one-dimensional steady field equation which exhibited smooth structured waves, acceleration waves, and shock waves. Subsequently, Greenberg [22] showed that steady shock wave solutions may exist for a large class of nonlinear materials with fading memory.‖ The concept of the propagation of steady waves in dissipative materials is extremely important to the present discussion and it is worthwhile to consider the results of Pipkin and Greenberg in some detail.

The motion is said to be *steady* if the displacement u can be represented by

$$u(X, t) = \hat{u}(\xi) \tag{3.24}$$

where $\xi = t - X/V$ and $V > 0$ is a given steady wave velocity. Then, by (2.1) and (3.24), the corresponding particle velocity and strain become

$$v(\xi) = \hat{u}'(\xi), \qquad \varepsilon(\xi) = \frac{1}{V}\hat{u}'(\xi) = \frac{1}{V}v(\xi). \tag{3.25}$$

A steady strain field implies, through (3.1), a steady stress field. Thus, if natural equilibrium conditions ($\sigma = 0, \varepsilon = 0$) exist far ahead of the wave, the momentum equation (2.3) reduces to

$$\sigma(\xi) = \rho_R V v(\xi) = \rho_R V^2 \varepsilon(\xi) \tag{3.26}$$

which holds for all ξ. Equations (3.26) and (3.1) combine to yield the functional equation

$$\rho_R V^2 \varepsilon(\xi) = \mathscr{S}(\varepsilon(\xi - s)) \tag{3.27}$$

for the steady strain field $\varepsilon(\xi)$.

† This is exactly the same type of behavior predicted by the linear theory of viscoelasticity. In this theory, the attenuation of shock and acceleration waves obey the same formula. Cf. Lee and Kanter [18], Chu [19], Coleman and Gurtin [2], Valanis [20].

‡ Note that the limit as $v^- \to 0$ is the same as the limit as $\varepsilon^- \to 0$.

§ Cf. Chen and Gurtin [13].

‖ Greenberg [23] also provided similar proofs for Maxwellian materials.

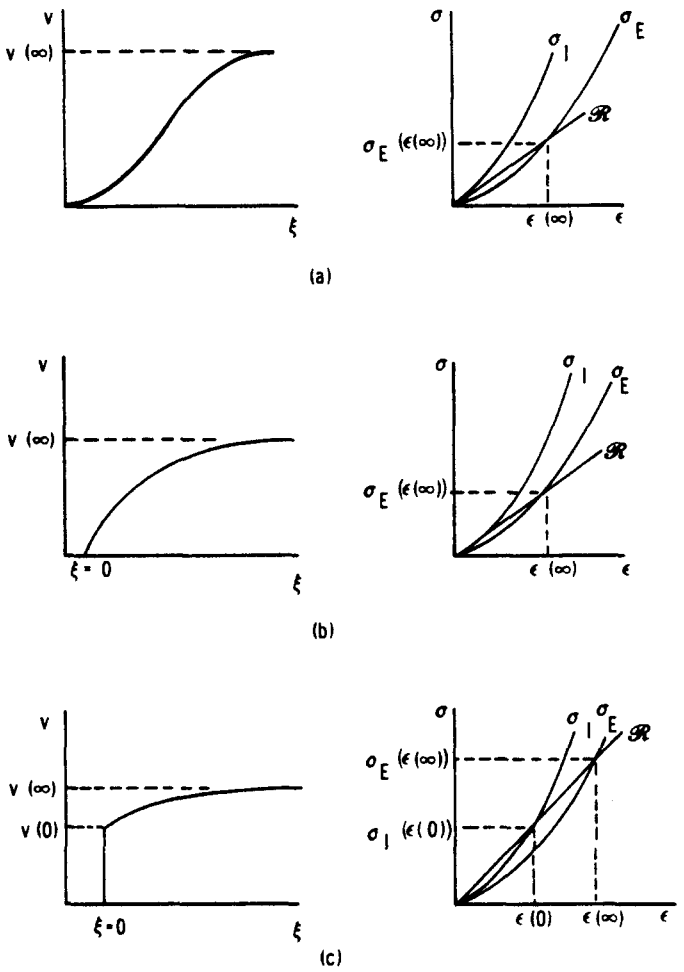

FIG. 1. Steady wave solutions.

We wish to consider the existence of solutions $\varepsilon(\xi)$, $0 < \varepsilon < 1$, of (3.27) which are monotone increasing functions of ξ. Greenberg [22] gave sufficient conditions for the existence of such solutions which are in essence the curvature conditions (3.8) and (3.9) and the requirement that the instantaneous longitudinal sound speed C_I, given by†

$$\rho_R C_I^2 = \hat{\partial}_\varepsilon \mathscr{S}(\varepsilon(\xi - s)),$$

must be monotone increasing as ξ increases. This latter requirement is to be expected on physical grounds. Intuitively, a steady wave in a nonlinear material with memory results from a balance being achieved between the tendency of the wave to decay due to internal dissipation (as manifested by $(3.9)_2$) and to grow due to nonlinear stress–strain response. Hence, in order to have a steady wave, each part of the wave must tend to overtake the part ahead of it. Clearly, this will result if the instantaneous sound speed C_I satisfies the monotonicity requirement.

† Note that $C_I = U$, the intrinsic velocity of an acceleration wave. Cf. Equation (3.10).

With these conditions, it can be shown that steady waves do indeed exist and that there are three types of solutions to consider which depend on the given steady wave velocity V:†

(i) $(C_I)_0 > V > (C_E)_0$,
(ii) $(C_I)_0 = V$,
(iii) $(C_I)_0 < V$,

where $(C_I)_0$ and $(C_E)_0$ are the instantaneous and equilibrium sound speeds corresponding to the natural equilibrium state, i.e.,

$$\rho_R(C_I)_0^2 = \left.\frac{d\sigma_I(\varepsilon)}{d\varepsilon}\right|_{\varepsilon=0}, \qquad \rho_R(C_E)_0^2 = \left.\frac{d\sigma_E(\varepsilon)}{d\varepsilon}\right|_{\varepsilon=0}. \tag{3.28}$$

Now, from (3.26), each point in a steady wave lies on a secant (Rayleigh line) in the stress–strain plane connecting the initial and final states. The slope of the Rayleigh line $\mathscr{R}$ is $\rho_R V^2$. Thus, the type of solution depends upon the position of the Rayleigh line with respect to the instantaneous and equilibrium stress–strain curves, $\sigma_I(\varepsilon)$ and $\sigma_E(\varepsilon)$ (See Fig. 1). In case (i), the Rayleigh line lies below the instantaneous curve (Fig. 1a). Then there exists a solution satisfying the conditions far ahead of the wave and the solution is a smooth structured wave with the final equilibrium particle velocity $v(\infty)$ (and strain $\varepsilon(\infty)$) obeying

$$\rho_R V^2 \varepsilon(\infty) = \sigma_E(\varepsilon(\infty)), \qquad v(\infty) = V\varepsilon(\infty). \tag{3.29}$$

Case (ii) corresponds to the Rayleigh line $\mathscr{R}$ tangent to the instantaneous curve (Fig. 1b). Thus, the steady wave velocity is the acceleration wave velocity and the solution is an acceleration wave with $\varepsilon(\infty)$, $v(\infty)$ satisfying (3.29). Case (iii) is of particular importance in this article and corresponds to a Rayleigh line with a slope greater than the initial slope of the instantaneous curve (Fig. 1c). In this instance, the equilibrium conditions far ahead of the wave can be satisfied only if $v(\xi) \equiv 0$, $\varepsilon(\xi) \equiv 0$ for $\xi < 0$ and there is a jump discontinuity in v (and ε) at $\xi = 0$ with $v(0)$, $\varepsilon(0)$ satisfying

$$\rho_R V^2 \varepsilon(0) = \sigma_I(\varepsilon(0)), \qquad v(0) = V\varepsilon(0). \tag{3.30}$$

This solution is a steady shock wave with the particle velocity (and strain) undergoing a smooth transition from $v(0)$ to $v(\infty)$ given by (3.29). Due to the monotonicity of the solution, $v(\infty) > v(0)$, $\varepsilon(\infty) > \varepsilon(0)$.

It has been found by Barker and Hollenbach [24] and Schuler [25] that steady shock waves can indeed be generated and observed in viscoelastic materials in plate-impact experiments. The techniques involved in performing such experiments will be considered in the next section.

4. EXPERIMENTAL TECHNIQUES

To study the evolutionary behavior of shock waves in viscoelastic materials, Barker and Hollenbach [24] and Schuler [25] have used a gas gun [26, 27] to produce a planar impact between two plates. The experimental configuration is shown in Fig. 2(a). Alternate target and projectile constructions which have been used to study acceleration wave and thin pulse propagation are shown in Figs. 2(b) and 2(c), respectively. The particulars of these arrangements will be discussed later in Sections 6.2 and 7.2. In each case

† Cf. Pipkin [21], Greenberg [22].

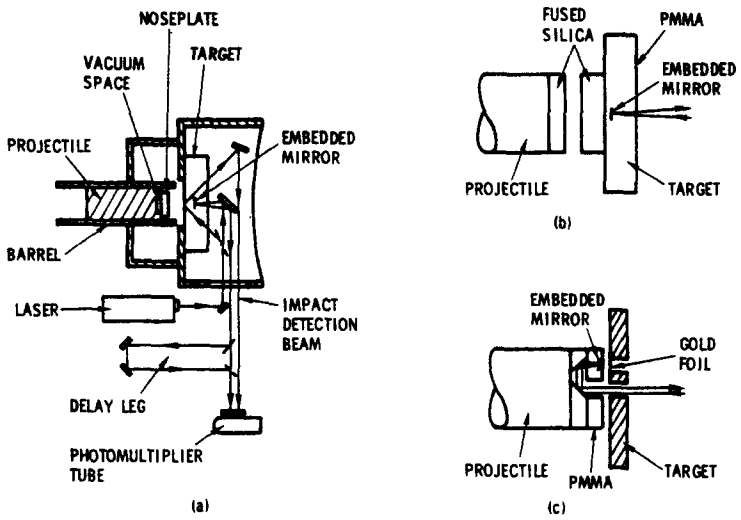

FIG. 2. Experimental configurations.

the experiments were designed such that the observation of the resulting wave profiles along the centerline of the target plate is completed before the arrival of unloading waves from the lateral surfaces of the target. If the material is isotropic, symmetry requires the motion during the time of observation to be that of one-dimensional stretch and hence, *purely longitudinal*. Hence, in rectangular Cartesian coordinates, the displacement is of the form

$$u_1 = u(X, t), \qquad u_2 = 0, \qquad u_3 = 0 \tag{4.1}$$

where the function u gives the displacement in the direction normal to the plane wave front of the material particle which occupied the position X in the homogeneous reference configuration. Thus, in the analysis of these experiments the one-dimensional theory presented in Sections 2 and 3 can be applied. All of the experimental data reported here were obtained on polymethyl methacrylate (PMMA) samples cut from sheets of Rohm and Haas Type II UVA Plexiglas ($\rho_R = 1{\cdot}185\ \mathrm{g/cm^3}$). Nevertheless, the experimental techniques described here can be applied, with certain modifications, to other polymeric materials.

In the plate-impact experiment, the gun barrel, expansion chamber, and target chamber are evacuated to less than 10^{-2} Torr prior to launching the projectile to prevent any detectable build up of air pressure between the projectile and target. The misalignment between the projectile nose piece and the target is minimized by employing the optical alignment technique described by Barker and Hollenbach [26]. The resulting tilt (angle between wave normal and sample surface) of the shock wave in the PMMA is less than 1°. Projectile velocities are measured to better than 0·1 per cent by using an electrically charged pin technique.

The target is fabricated from two or more disks of the sample material. A thin aluminum mirror typically 100 nm thick and 12 mm in diameter is vapor-deposited on the surface in the center of one of the disks; the disks are then joined by a thin (<0·02 mm) layer of

epoxy cement. Since the density and dynamic mechanical behavior of epoxy is close to that of PMMA, the epoxy has negligible effect on the measured wave shape. The shock impedance of the aluminum mirror is significantly different from that of PMMA; however, because of its thinness, the mirror reaches equilibrium with its surroundings in a fraction of a nanosecond. Thus measurement of the velocity of the mirror is essentially a direct measurement of the particle velocity in the PMMA.

For the measurement of particle velocities below 0·06 mm/μsec, a Michelson type interferometer, described by Barker and Hollenbach [27], is employed. The displacement history of the embedded mirror recorded by this interferometer is numerically differentiated to yield velocity. For higher particle velocities, the velocity interferometer developed by Barker [28] is used. This interferometer (Fig. 2a) introduces a delay leg into a laser beam which is reflected from the moving embedded mirror. Thus, at the photomultiplier tube two images of the mirror, initially separated by the length of the delay leg, are superimposed. As the mirror moves the separation distance between these images changes. For each half wavelength change in separation distance a complete cycle of constructive-destructive interference of the light beam is observed by the photomultiplier tube. It is easily shown [24] that the number of interference cycles (fringes) N is related to the velocity through

$$v(t) = \frac{\lambda_0}{2\tau_L} N(t). \tag{4.2}$$

where λ_0 is the wavelength of the laser light and τ_L is the time it takes light to traverse the delay leg.

The time at which the centers of the target and projectile plates impact is determined using an optical technique. A small fraction of the incoming laser beam is split off and directed to undergo total internal reflection at the center of the impact surface (Fig. 2a). At impact, the beam is lost by transmission through the projectile nose plate. The time at which the resulting intensity loss occurs can be easily resolved to a few nanoseconds. From knowledge of this time, the time at which the shock arrives at the mirror, and the distance from the impact surface to the mirror, an average shock velocity may be calculated with an uncertainty of about 1 per cent.

After the shock wave has passed the mirror, it produces a region of compression between it and the mirror in which the index of refraction differs from that of the uncompressed material. The light beam monitoring the motion of the mirror is affected by this change in index of refraction. In reducing the data from both the velocity and displacement interferometer, this effect must be taken into account. Barker and Hollenbach [24] report that in PMMA over the range of stress considered here a maximum correction of 1·1 per cent must be applied to particle velocity measurements. With these corrections, the estimated error in particle velocity measurement is at most 5 per cent.

A typical particle velocity history in PMMA is shown in Fig. 3. This record was obtained by impacting a 6·568 mm thick projectile nose plate into a target at 0·45 mm/μsec and observing the wave form 6·359 mm from the impact surface. It can be seen that the profile consists of a shock, in which the particle velocity jumps to a value v_0, followed by a smooth transition to a maximum particle velocity v_∞. At t_b an unloading wave which is produced by the reflection of the compressive wave from the free surface of the projectile nose plate arrives at the mirror and reduces the particle velocity.

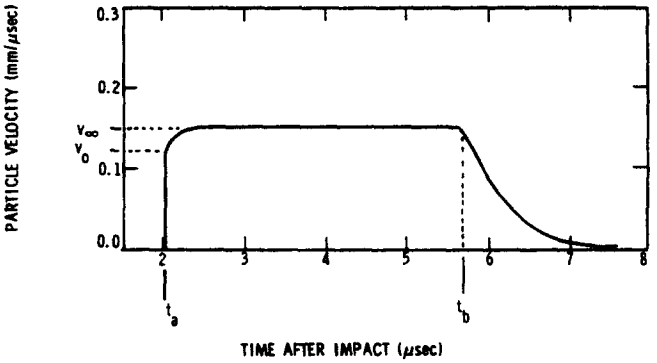

FIG. 3. Typical particle velocity profile.

5. ANALYSIS OF STEADY SHOCK WAVES

5.1 *Results of experimental studies*

Using the experimental technique described in the previous section, Barker and Hollenbach [24] and Schuler [25] have generated and observed steady shock waves in the solid polymer, PMMA. Their data are summarized in Table 1 and the measured particle velocity histories corresponding to the impact conditions of 0·06, 0·15 and 0·3 mm/μsec are shown in Fig. 4. The records of the 0·06 mm/μsec impact condition show a noticeable decay in the strength of the shock front and an accompanying smoothing of the wave shape with increasing distance of propagation. For the 0·15 mm/μsec impact condition, the particle velocity histories measured at 6, 12 and 37 mm from the impact surface are nearly identical. Thus, it appears that within 6 mm from the impact surface, the wave generated at this impact condition becomes steady. The particle velocity records for the 0·3 mm/μsec impact condition indicate that a similar steady wave form has been achieved.

Now, from the analysis of steady waves (Section 3.4), it is evident that measurement of the steady wave velocity V and the particle velocity jump at the front v_0 for various impact levels serves to determine the instantaneous response of the material, while measurement of V and the maximum equilibrium particle velocity v_∞ achieved for various impact levels serves to determine the equilibrium response of the material. Thus, from a series of steady wave experiments, two curves are generated in the wave velocity–particle velocity plane, "$V-v_0$" and "$V-v_\infty$". Consequently, for every value of particle velocity v, we can identify two wave velocities, $V_I(v)$ and $V_E(v)$. These curves may be represented by least squares, polynomial fits of the experimental data. In the case of PMMA,†

$$V_I(v) = (C_I)_0 + b_I v + a_I v^2, \tag{5.1}$$

$$V_E(v) = (C_E)_0 + b_E v + a_E v^2. \tag{5.2}$$

Figure 5(a) shows the data for PMMA and fits (5.1) and (5.2). The value of the instantaneous longitudinal sound speed $(C_I)_0$ in the fit (5.1) agrees with the ultrasonic longitudinal wave speed measured by Asay, Lamberson and Guenther [29].‡ Although the equilibrium

† The coefficients for PMMA for $v < 0{\cdot}3$ mm/μsec are: $(C_I)_0 = 2{\cdot}76$ mm/μsec, $b_I = 3{\cdot}62$, $a_I = -5{\cdot}64$ μsec/mm, $(C_E)_0 = 2{\cdot}74$ mm/μsec, $b_E = 3{\cdot}50$, $a_E = -6{\cdot}89$ μsec/mm. Cf. Schuler [25].

‡ The equivalence of the instantaneous sound speed $(C_I)_0$ and the ultrasonic wave speed was established by Coleman and Gurtin [2] for general nonlinear materials with memory. From the acoustic experiments on PMMA [29], $(C_I)_0 = 2{\cdot}765$ mm/μsec.

TABLE 1. SHOCK WAVE MEASUREMENTS IN PMMA [24, 25]

Nominal impact velocity (mm/μsec)	Shot number	Actual impact velocity v_m (mm/μsec)	Mirror distance X_m(mm)	Shock velocity (mm/μsec)	Unloading wave velocity (mm/μsec)	Particle velocity jump at shock v_0(mm/μsec)	Maximum particle velocity $v_m/2 = v_\infty$ (mm/μsec)
0·06	312	0·0609	6·349	2·843	2·97	0·0245	0·0305
	313	0·0613	6·284	2·844	2·96	0·0245	0·0306
	2109	0·0617	19·163	2·838	2·97	0·0240	0·0308
	2105	0·0617	37·452	2·834	2·95	0·0190	0·0306
0·15	314	0·1511	6·185	2·968	3·21	0·062	0·0756
	315	0·1516	6·388	2·959	3·22	0·065	0·0758
	2110	0·1511	12·824	2·974	3·22	0·061	0·0756
	2112	0·1547	12·898	2·958	3·22	0·057	0·0773
	2115	0·1514	37·539	2·991	3·23	0·060	0·0757
0·22	2119	0·2236	36·504	3·032	3·34	0·091	0·1118
0·30	316	0·3085	6·208	3·127	3·53	0·126	0·1542
	317	0·3090	6·160	3·130	3·54	0·127	0·1545
	2113	0·2999	25·252	3·113	3·51	0·122	0·1499
	2116	0·2985	37·283	3·106	3·49	0·122	0·1492
0·46	2106R	0·4501	6·359	3·199	3·78	0·160	0·2250
	2107R1	0·4604	25·314	3·178	3·76	0·150	0·2301
	2107R2	0·4616	37·903	3·181	3·73	0·152	0·2307
0·64	318	0·6412	6·045	3·268	4·20	0·210	0·3206
	319	0·6391	6·116	3·268	4·18	0·205	0·3159
	2104	0·6431	18·782	3·249	—	0·175	0·3216
	2108	0·6217	25·189	3·199	4·07	0·162	0·3108
	2111	0·6165	37·490	3·203	—	0·161	0·3082
0·64	320	0·6092	6·269	3·349	4·84	0·300	—
	321	0·6147	6·350	3·342	4·87	0·315	—

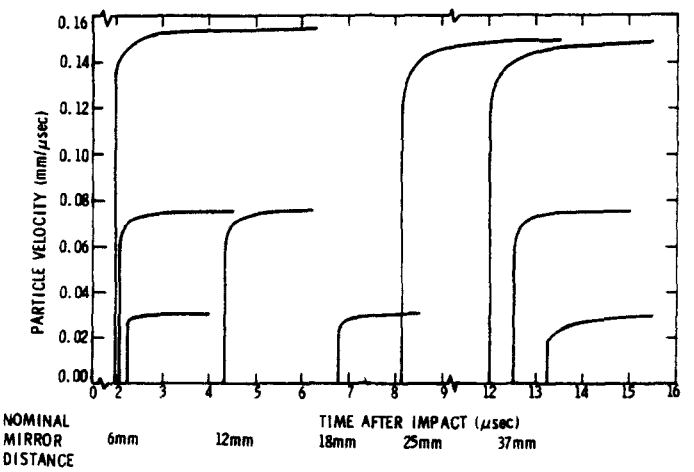

FIG. 4. Particle velocity histories.

longitudinal sound speed cannot be measured directly in acoustic experiments, Nunziato and Sutherland [30] have suggested a method by which it can be determined from acoustic dispersion data. The value of $(C_E)_0$ they deduced for PMMA agrees favorably with the value in the fit (5.2).†

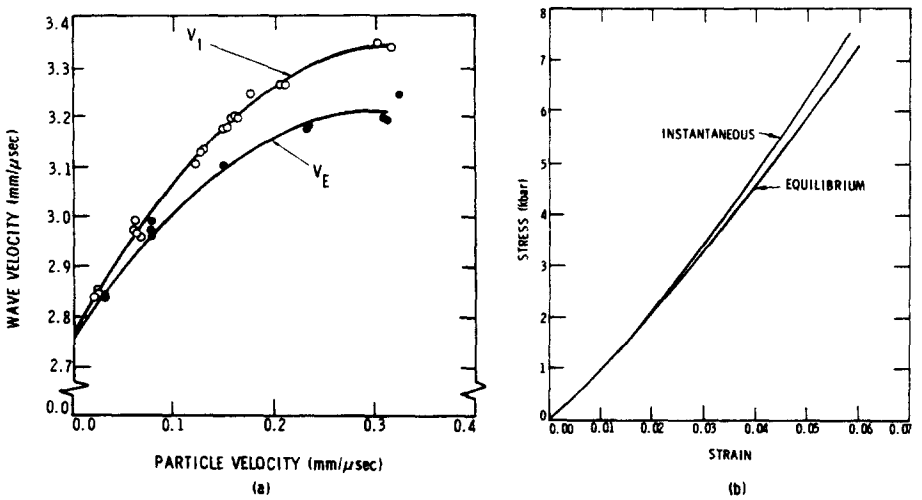

FIG. 5. Steady wave velocity–particle velocity curves/instantaneous and equilibrium stress–strain curves.

5.2 *Constitutive model and response functions*

In order to analyze the steady wave profiles observed in PMMA, it is necessary to assume a specific constitutive model for the material. Following Pipkin [21], Schuler [25] assumed that the stress functional $\mathscr{S}$ could be represented by the one-dimensional counterpart of the constitutive equation of *finite linear viscoelasticity* developed by Coleman and Noll [4]:

$$\sigma(t) = \mathscr{S}(\varepsilon^t) = \sigma_I(\varepsilon(t)) + \int_0^\infty \hat{G}'(\varepsilon; s)\{1-(1-\varepsilon^t(s))^2\}\,ds \tag{5.3}$$

for all compressive strain histories $\varepsilon^t(s)$.‡ The relaxation function $\hat{G}'(\varepsilon; s)$ has the property $\lim_{s\to\infty} \hat{G}'(\cdot, s) = 0$. Evaluating (5.3) for the equilibrium history $\varepsilon_E(s)$, $0 \le s < \infty$, it follows that the instantaneous and equilibrium response functions are related by

$$\sigma_I(\varepsilon) = \sigma_E(\varepsilon) + [\hat{G}(\varepsilon; 0) - \hat{G}(\varepsilon; \infty)]\{1-(1-\varepsilon)^2\}. \tag{5.4}$$

Now, from the measurements of the steady wave velocity and the particle velocity at the head and at the tail of the steady wave the instantaneous and equilibrium response functions, $\sigma_I(\varepsilon)$ and $\sigma_E(\varepsilon)$, can be uniquely determined. Using (5.1) and (5.2), along with

† From acoustic dispersion data [30], $(C_E)_0 = 2{\cdot}728$ mm/μsec.

‡ Cf. Herrmann and Nunziato [31] for this particular form of the finite linear viscoelastic constitutive equation.

$(3.29)_2$ and $(3.30)_2$, the velocities V_I and V_E can alternatively be expressed in terms of strain:

$$V_I(\varepsilon) = \frac{\hat{b}_I - [\hat{b}_I - 4(C_I)_0 a_I \varepsilon^2]^{\ddagger}}{2a_I\varepsilon^2},$$
$$V_E(\varepsilon) = \frac{\hat{b}_E - [\hat{b}_E - 4(C_E)_0 a_E \varepsilon^2]^{\ddagger}}{2a_E\varepsilon^2}, \tag{5.5}$$

where $\hat{b}_I = 1 - b_I\varepsilon$, $\hat{b}_E = 1 - b_E\varepsilon$. Then, it follows from $(3.29)_1$ and $(3.30)_1$, that

$$\sigma_I(\varepsilon) = \rho_R V_I^2(\varepsilon)\varepsilon, \qquad \sigma_E(\varepsilon) = \rho_R V_E^2(\varepsilon)\varepsilon. \tag{5.6}$$

The instantaneous and equilibrium stress–strain curves for PMMA are shown in Fig. 5(b).

In order to proceed further, some assumption must be made with regard to the form of $\hat{G}(\varepsilon; s)$. Consistent with the assumptions made by Pipkin [21] and Greenberg [22] to insure the existence of steady waves, Schuler [25] assumed that

$$\hat{G}(\varepsilon; s) = [\hat{G}(\varepsilon; 0) - \hat{G}(\varepsilon; \infty)] \exp\left(-\frac{s}{\tau}\right) + \hat{G}(\varepsilon; \infty). \tag{5.7}$$

where $\tau > 0$ is a constant relaxation time.† A recent analysis of acoustic dispersion data by Nunziato and Sutherland [30] has shown that a single exponential relaxation function of this type is indeed appropriate for shock wave propagation in PMMA, even though three decades of time may be involved in such experiments.

5.3 *Steady shock wave solutions*

Using the stress functional given by (5.3), we may obtain steady wave solutions of (3.27) which contain a shock discontinuity (type (iii) of Section 3.4). In particular, equations (3.27), (5.3), (5.4) and (5.7) combine to yield the integral equation

$$\frac{\sigma_I(\varepsilon) - \rho_R V^2 \varepsilon}{\sigma_I(\varepsilon) - \sigma_E(\varepsilon)} = \frac{1}{\tau}\int_0^{\infty} \exp\left(-\frac{s}{\tau}\right) \frac{\{1-(1-\varepsilon(\xi-s))^2\}}{\{1-(1-\varepsilon(\xi))^2\}}\, ds \tag{5.8}$$

for the steady strain field $\varepsilon(\xi)$. With (5.5) and (5.6), this equation can be solved by differentiating with respect to ξ and then integrating the resulting first-order differential equation by quadrature.‡ Using (3.25) to express the result in terms of particle velocity, the solution of (5.8) is

$$\frac{\xi - \xi_0}{\tau} = -\ln\left\{\frac{V - (C_E)_0 - b_E v - a_E v^2}{(C_I)_0 - (C_E)_0 + (b_I - b_E)v + (a_I - a_E)v^2}\right\}$$
$$+ \xi_1 \ln|v - v_1| + \xi_2 \ln|v - v_2| + \xi_3 \ln|v| + \xi_4 \ln|2V - v| \tag{5.9}$$

where v_1 and v_2 are the solutions of the quadratic

$$a_E v^2 + b_E v + (C_E)_0 - V = 0, \tag{5.10}$$

† Finite linear viscoelastic materials with the relaxation function (5.7) are also Maxwellian; cf. Herrmann and Nunziato [31].

‡ Cf. Pipkin [21], Schuler [25].

and $\xi_0, \xi_1, \xi_2, \xi_3, \xi_4$ are constants given by

$$\xi_1 = -\frac{2[(C_I)_0 - V + b_I v_1 + a_I v_1^2](V - v_1)}{a_E(v_2 - v_1)v_1(2V - v_1)},$$

$$\xi_2 = -\frac{2[(C_I)_0 - V + b_I v_2 + a_I v_2^2](V - v_2)}{a_E(v_2 - v_1)v_2(2V - v_2)},$$

$$\xi_3 = -\frac{V - (C_I)_0}{V - (C_E)_0}, \qquad \xi_4 = \frac{[(C_I)_0 - V + 2b_I V + 4a_I V^2]}{a_E(2V - v_1)(2V - v_2)}.$$

Now, for the solution to be that of a steady shock wave, $V > (C_I)_0$. In this instance, $\xi_3 < 0$ and the equilibrium conditions far ahead of the wave (i.e., v vanishes as $\xi \to -\infty$) can be satisfied only if $v \equiv 0$ for $\xi < 0$ and there is a jump discontinuity in v at $\xi = 0$ with $v(0)$ the smallest positive root of

$$a_I v^2 + b_I v + (C_I)_0 - V = 0. \tag{5.11}$$

The maximum particle velocity achieved, $v(\infty)$, is the smallest positive root of (5.10).†

To compare the predicted steady shock wave solutions (5.9) with the experimentally observed wave profiles, it remains to specify the relaxation time τ. For each specified impact condition, the steady wave velocity V is known and the wave profile can be calculated as a function of the non-dimensional parameter $(\xi - \xi_0)/\tau$. In each case a relaxation time can be determined such that the particle velocity half-way between the jump at the shock v_0 and the maximum v_∞ occurred at a time commensurate with the data. Using this approach, Schuler [25] obtained an average relaxation time τ for PMMA. Schuler's result compares favorably with the relaxation time deduced by Nunziato and Sutherland [30] from acoustic data.‡

Generally, it is difficult to make good comparisons of calculated wave profiles with observed wave profiles. This is primarily due to the fact that for a given steady wave velocity the values of the particle velocity jump at the shock and the maximum particle velocity calculated using the polynomial fits (5.1) and (5.2) will not in general be commensurate with those actually observed. Thus, in making the calculations shown in Fig. 6 for PMMA, Schuler [25] made slight adjustments in the steady wave velocity V to give the best agreement at the wave front and at the tail of the wave. The comparisons shown correspond to wave profiles experimentally observed at propagation distances greater than 37 mm. The lower profile corresponds to an impact condition of 0·30 mm/μsec and a measured steady wave velocity of 3·106 mm/μsec; while the upper profile corresponds to an impact condition of 0·15 mm/μsec and a shock velocity of 2·991 mm/μsec. The steady wave velocity used by Schuler [25] in the calculations was 3·106 and 2·965 mm/μsec, respectively. It is seen that good agreement was obtained, particularly for the 0·15 mm/μsec impact condition.

The calculated profiles shown in Fig. 6 were obtained using (5.9) which is a necessary condition for a steady wave. However, the waveforms must also satisfy the sufficiency requirement based on the sound speed criterion discussed in Section 3.4. Schuler [25] has shown that this criterion is indeed satisfied for the profiles shown. However, for impact conditions greater than 0·30 mm/μsec (about 7·5 kbar), this criterion is not satisfied. At

† The values $v(0)$ and $v(\infty)$ correspond to v_0 and v_∞, respectively, in Fig. 3.

‡ Schuler [25] obtained $\tau \approx 0{\cdot}25$ μsec; while Nunziato and Sutherland [30] found that $\tau = 0{\cdot}22$ μsec.

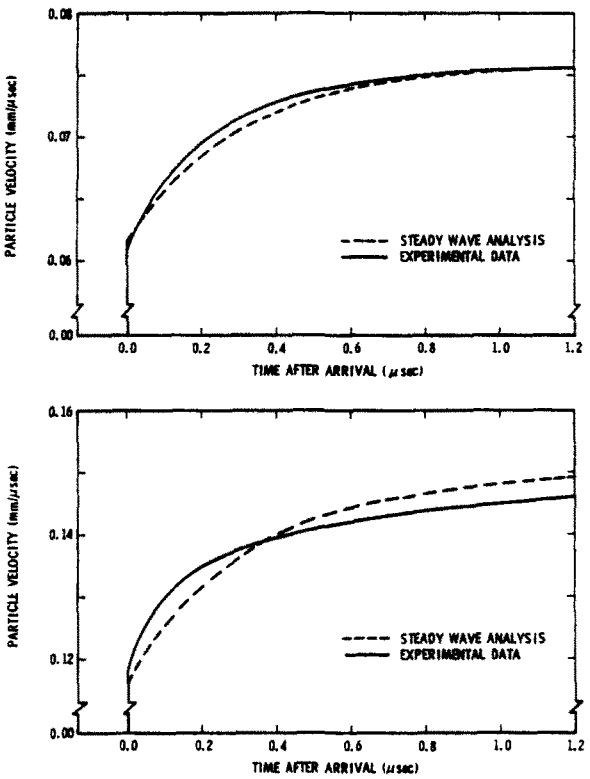

FIG. 6. Comparison of observed and calculated steady wave profiles.

this stress level, Schuler [25, 32] and Barker and Hollenbach [24] have detected an inflection in the equilibrium stress–strain curve of PMMA. This observation suggests that the finite linear viscoelastic constitutive assumption used here is only valid for PMMA up to this level of stress. A characterization of the dynamic viscoelastic response of PMMA above 7·5 kbar has been considered by Schuler and Nunziato [33].

6. GROWTH AND DECAY OF SHOCK WAVES

Two applications of the amplitude equation for shock waves are considered in this section. First, the concept of the critical acceleration is discussed for a particular viscoelastic model. Then, an approximate technique is described which permits the shock amplitude equation to be used to predict the attenuation of thin shock pulses.

6.1 *The critical acceleration*

In the general discussion of shock waves in materials with memory (Section 3.3), it was shown that the growth and decay behavior of a wave propagating into a region unstrained for all past times depends on the relative magnitude of the particle acceleration immediately behind the shock $(\dot{v})^-$ and the critical acceleration

$$U^2|\hat{\lambda}| = \frac{U|G'(\varepsilon^-;0)|\varepsilon^-}{E_I^-(1-\hat{\mu})}, \tag{6.1}$$

where $\hat{\mu} < 1$ is defined by (3.18). The critical acceleration depends upon the strain (or particle velocity) both explicitly and through the strain dependence of the shock velocity U, the instantaneous tangent modulus E_I and the initial slope of the relaxation function $G'(\varepsilon^-;0)$. Hence, to obtain $\hat{\lambda}(\varepsilon^-)$ for a particular material it is necessary to determine the strain dependence of these functions from experimental measurements. Here, following the study of Schuler and Walsh [34], this critical acceleration is determined for a particular constitutive model and the results compared to experimental shock propagation studies involving the solid polymer, PMMA.

As described in Section 5.2 the strain dependence of the shock velocity† is obtained directly from the experimental measurements which yield the shock velocity–particle velocity dependence. Further, from the results of the steady wave studies, in particular equations $(3.5)_1$, $(5.5)_1$ and $(5.6)_1$, the strain dependence of the instantaneous tangent modulus can be obtained. This leaves the function $G'(\varepsilon^-;0)$ to be determined. As one would expect, this function can be determined from the measured instantaneous and equilibrium response functions and the relaxation time τ.

To show this, we consider the constitutive relation (5.3) for finite linear viscoelastic materials with $\hat{G}(\varepsilon;s)$ represented by (5.7). Then, (5.3) becomes

$$\sigma(t) = \sigma_I(\varepsilon(t)) - \frac{1}{\tau}\int_0^\infty \left\{[G(\varepsilon;0) - G(\varepsilon;\infty)]\exp\left(-\frac{s}{\tau}\right)\right\}\{1-(1-\varepsilon^t(s))^2\}\,\mathrm{d}s. \tag{6.2}$$

The response functions involved in the definition of the critical acceleration have been associated with the constitutive assumption (3.1) for materials with memory. To relate (6.2) to this general model it is necessary to compute the derivative of equation (6.2) with respect to an arbitrary strain history and then evaluate this result for the appropriate reference history; i.e. in the case of the shock wave studies, with respect to the jump history (3.4). Thus, for equation (6.2), we calculate

$$\mathscr{S}'(\varepsilon^t;\gamma^t) = \frac{\mathrm{d}}{\mathrm{d}\alpha}\mathscr{S}(\varepsilon^t + \alpha\gamma^t)|_{\alpha=0}$$

and evaluate the resulting equation for $\varepsilon^t(s) = \varepsilon_I(s)$. Carrying this through and comparing with (3.3) it follows that

$$G_I(0) = \left.\frac{\mathrm{d}\sigma_I(\varepsilon)}{\mathrm{d}\varepsilon}\right|_{\varepsilon=\varepsilon^-}, \qquad G_I'(s) = 2\hat{G}'(\varepsilon^-;s).$$

Combining this with (5.7) and using (5.4) yields

$$G'(\varepsilon^-;0) = -\frac{2}{\varepsilon^-(2-\varepsilon^-)\tau}[\sigma_I(\varepsilon^-) - \sigma_E(\varepsilon^-)] \tag{6.3}$$

when evaluated at $s = 0$.

With $U(\varepsilon^-)$, $E_I(\varepsilon^-)$ and $G'(\varepsilon^-;0)$ known, the calculation of $U^2(\varepsilon^-)|\hat{\lambda}(\varepsilon^-)|$ is carried out using (6.1). Actually, in presenting the results for PMMA we follow the lead indicated earlier and determine the critical acceleration $U^2|\hat{\lambda}|$ as a function of the particle velocity behind the shock. Figure 7 shows this dependence as the dashed line along with the ranges of values of $U^2|\hat{\lambda}| = (\dot{v})^-$ determined graphically from the experimental steady wave profiles at three impact levels. The error brackets reflect not only the difference between

† Note that $V_I(\varepsilon^-) = U(\varepsilon^-)$.

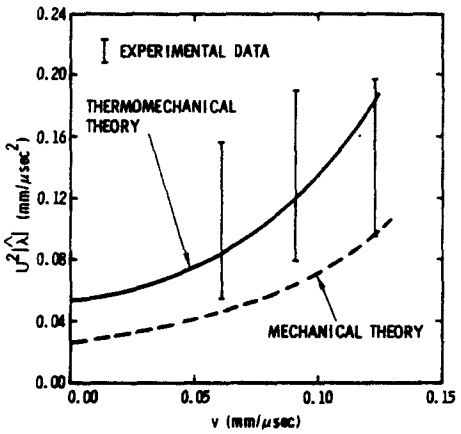

FIG. 7. Comparison of observed and calculated critical acceleration.

the results for several experiments at the same nominal impact level, but also the uncertainties in determination of the slopes. In view of the extreme sensitivity of the calculated values of $U^2|\hat{\lambda}|$ to variations in the fits for σ_I and σ_E and the relaxation time τ, the correlation appears to give at least a qualitative verification of the concept of a critical acceleration and of the methods of obtaining material response functions from experimental shock wave studies.

Of course, the continued growth or decay of the shock front cannot be predicted solely from these results. That is, as the jump in particle velocity varies, the particle acceleration immediately behind the front will in general change. From the dependence of $\hat{\lambda}$ on ε^- (and hence on v^-), the value of the critical acceleration changes and, in turn, affects the rate of growth or decay of the wave through (3.22). This has been considered by Chen, Gurtin and Walsh [35] in a study of the long-range amplitude behavior assuming $(\partial_X \varepsilon)^-$ is constant.

6.2 *Shock pulse attenuation*

As has been mentioned previously, the shock amplitude equation (3.22) cannot in general be used to determine $v^-(t)$ since the particle acceleration $(\dot{v})^-(t)$ is not known in advance. However, Nunziato and Schuler [36] have recently shown that (3.22) can be used to evaluate $v^-(t)$ for a certain type of shock wave problem, called the thin pulse problem, by approximating $(\dot{v})^-(t)$. The problem is one of calculating the attenuation of a pulse which consists of a shock front propagating into an unstrained region at rest followed immediately by an unloading wave of arbitrary shape which unloads the material to its original unstressed state (Fig. 8). Here we follow the approach of Nunziato and Schuler to calculate the attenuation of a thin shock pulse in PMMA and compare the results with experimental observations.

For viscoelastic materials, the shock loads the material along a Rayleigh line to a point on the instantaneous stress–strain curve $\sigma_I(\varepsilon^-)$, and the unloading wave unloads it along some unknown stress–strain path. This unloading path will always be between the instantaneous and equilibrium stress–strain curves. However, for thin pulses the strain rates, particularly in the initial portion of the unloading wave, are very high. At such high strain rates, the behavior of the material is primarily governed by the instantaneous

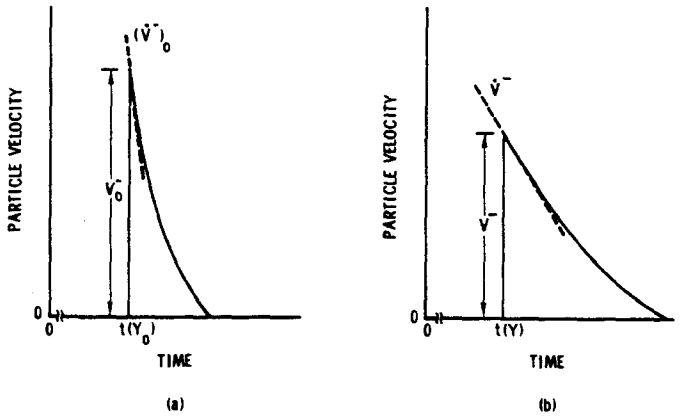

(a) (b)

FIG. 8. Thin pulse profiles.

elasticity of the material. Thus, it is assumed that the unloading stress–strain path is the instantaneous stress–strain curve σ_I.

This assumption means that the effects of rate-dependence on the unloading wave are neglected and the unloading wave is treated as a wave propagating in a nonlinear elastic material whose stress–strain curve is $\sigma_I(\varepsilon)$.† Furthermore the following simplifying assumptions will be made concerning the unloading wave:

(i) the unloading wave is a simple wave, and

(ii) the unloading path in the stress–particle velocity plane is the instantaneous curve, $\sigma_{IH}(v^-)$, determined by $(2.10)_1$.

Assumption (ii) is an approximation which eliminates the reflection of the unloading wave from the shock wave and hence insures that the unloading wave remains a simple wave for all time. This approximation should prove to be especially good for shocks of weak to moderate strength.

The assumption (ii) gives a one-to-one correspondence between points on the unloading wave and points on the instantaneous stress–particle velocity curve over the corresponding range of particle velocity. Furthermore from assumption (i) each point on the unloading wave propagates at a constant level of particle velocity with the corresponding *intrinsic instantaneous sound speed* $C_I = (E_I/\rho_R)^{\frac{1}{2}}$. Let the smooth function $t_0(v)$ represent the initial unloading wave profile at the material point Y_0 (Fig. 8a). Then the unloading portion of the subsequent profile (Fig. 8b) can also be represented by the smooth function $t(v)$ which is related to the initial profile $t_0(v)$ through the simple wave relation‡

$$t(v) = t_0(v) + \frac{X - Y_0}{C_I(v)} \tag{6.4}$$

for each $v \leq v^-$ and for all material points $X \geq Y_0$.

Differentiating the simple wave description (6.4) with respect to v, inverting, and evaluating the result at the shock front yields the following expression for the particle

† Nevertheless, the effects of internal dissipation still enter the calculations through the critical acceleration term of (3.22).

‡ A similar representation of the unloading wave was employed by Bertholf and Oliver [37] and Fowles [38] in studies of attenuation in elastic materials. Their approach to the problem differs from that discussed here.

acceleration immediately behind the front:

$$(\dot{v})^- = \left(\frac{1}{(\dot{v})_0^-} - \left|\frac{dC_I(v)}{dv}\right|^- \frac{Y(t)-Y_0}{[C_I^2(v)]^-}\right)^{-1}.$$

Here, $Y(t) \geq Y_0$ is the location of the shock front at time t, and

$$(\dot{v})_0^- = \dot{v}_0(v^-) < 0$$

is the slope of the initial unloading wave profile at the particle velocity v^-. Substitution of this result in the viscoelastic shock amplitude equation (3.22) yields the ordinary differential equation

$$\frac{dv^-}{dt} = \xi_I(v^-)\left\{\frac{1}{\beta_I(v^-)-\alpha_I(v^-)[Y(t)-Y_0]} - U^2(v^-)|\hat{\lambda}(v^-)|\right\} \tag{6.5}$$

where we have set

$$\xi_I(v^-) = \frac{[1-\hat{\mu}^2(v^-)]}{[1+3\hat{\mu}(v^-)]}, \tag{6.6}$$

$$\beta_I(v^-) = \frac{1}{\dot{v}_0(v^-)}, \qquad \alpha_I(v^-) = \frac{1}{C_I^2(v^-)}\left|\frac{dC_I(v)}{dv}\right|^-, \tag{6.7}$$

and $U^2|\hat{\lambda}|$ is given by (6.1). Since $\xi_I(v^-) > 0, \alpha_I(v^-) > 0, \beta_I(v^-) < 0$ for all $v^- \neq 0$, it follows from (2.6) and (6.5) that the shock wave amplitude v^- in viscoelastic materials is monotone decreasing and will approach a limiting value (zero) in an infinite time.

Using (5.1) along with $(5.5)_1$, $(5.6)_1$, (2.9), (3.6), (3.18) and the results of the last section, all of the quantities appearing in (6.5), (6.6) and (6.7) may be determined in terms of the particle velocity v^-.

The experimental technique employed by Nunziato and Schuler [36] to generate and observe thin pulse propagation in viscoelastic materials is shown schematically in Fig. 2(c). The specimen through which the pulse propagation is to be observed in this case is attached to the nose of a projectile. The pulse is produced by the impact of the specimen against a thin (0.0216 mm) gold foil target. In a series of four experiments for which the impact velocity was 0·31 mm/μsec the pulse profile was observed at distances of 0·48, 1·26, 3·20 and 5·969 mm from the impact surface. Due to the impedance mismatch between the PMMA and gold, an unloading wave from the free surface of the foil reflects from the impact surface and only partially unloads the PMMA. The wave reflected back into the gold subsequently re-reflects at the gold's free surface, and thus establishes a reverberation pattern. This reverberation pattern makes it extremely difficult to determine the particle velocity–time profile at the point where attenuation begins. Therefore, the particle velocity history measured at the mirror distance $X_m = 0{\cdot}48$ mm was used as the initial pulse shape. From this data the initial unloading profile was fitted as†

$$t_0(v) = -k \ln\left(\frac{v}{v_0^-}\right), \qquad v \leq v_0^-. \tag{6.8}$$

With the initial pulse shape specified and the material response functions known, we can calculate the attenuation curve $v^-(X)$ by numerically integrating the differential equations (6.5) and (2.6). The resulting solution is compared with the experimental datum

† Here $k = 0{\cdot}134$ μsec and $v_0^- = 0{\cdot}26$ mm/μsec.

points in Fig. 9. Here the propagation distance X has been normalized with respect to the mirror location corresponding to the initial pulse. It is evident that the approximate solution compares well (± 5 per cent) with the experimentally observed attenuation of the shock amplitude. Since the impact velocity in the experiments was relatively low, reflections of the unloading wave from the shock wave were not expected to influence the attenuation and this is borne out in Fig. 9. By assuming unloading along the instantaneous curve, one would expect the predicted attenuation to be less than that observed. However, the good comparison in Fig. 9 seems to indicate that in these experiments the unloading stress–strain path does lie very close to the instantaneous curve.

Finally, from the simple wave description (6.4) and the initial pulse shape (6.8), we can determine the wave shape at any other point. The pulse shape was calculated for $X = 5{\cdot}489$ mm and compared with the particle's velocity–time history measured at that point. The results are shown in the inset of Fig. 9.

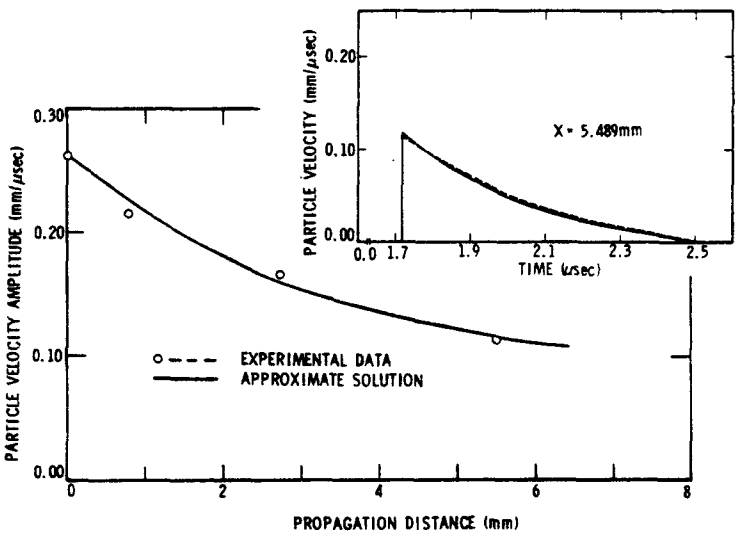

FIG. 9. Comparison of calculated and observed attenuation and pulse shape.

7. VELOCITY AND GROWTH OF ACCELERATION WAVES

In this section the equations governing the velocity and the growth and decay of acceleration waves are applied to two experimental situations. The first of these concerns a determination of the velocity of unloading wave fronts which are considered as expansive acceleration waves. The second concerns the velocity, growth and decay of compressive acceleration waves propagating into a region which is unstrained and at rest.

7.1 *Acceleration wave velocities*

It is evident from Fig. 3 that an unloading wave may be considered to be an expansive wave propagating into a deformed region. Here, following Schuler [32], the velocity of an unloading wave is calculated using the constitutive model of finite linear viscoelasticity

developed from the steady wave study. The results are compared with experimentally measured unloading wave velocities.

The velocity of an acceleration wave propagating in a finite linear viscoelastic material may be obtained by substituting equation (5.3) into (3.10) yielding

$$U^2 = \frac{1}{\rho_R}\left\{\frac{d\sigma_I(\varepsilon)}{d\varepsilon} + \int_0^\infty \frac{d}{d\varepsilon}\hat{G}'(\varepsilon; s)\{1-(1-\varepsilon^t(s))^2\}\, ds\right\}. \tag{7.1}$$

We note that in general the intrinsic velocity U is a function of the current strain state and the past history of the strain.

Ideally, in order to compare the predictions of (7.1) with the experimental observation of unloading waves, the following procedure should be followed: (a) determine the history of the deformation at particles through which the unloading wave passes and (b) use (7.1) to determine U as a function of time at each particle. Clearly, this procedure is difficult. For example, the deformation history experienced by a particle located at the free surface of the flyer plate consists of a sudden jump in strain caused by the arrival of the shock. Hence the acceleration wave velocity at this particle can be found from (7.1) by using the jump history (3.4). In contrast to what occurs at this position, a particle located at the impact surface has a relatively long time to reach equilibrium prior to the arrival of the unloading wave. If this particle does reach equilibrium, the appropriate history to employ in (7.1) is the equilibrium history, $\varepsilon_E(s) = \varepsilon$, $0 \le s < \infty$. At other particles in the path of the unloading wave, it is not clear what might be a reasonable history to assume. However, since the jump and equilibrium histories represent extremes, consideration of these two histories should provide bounds on the variation of the acceleration wave velocity.

For the jump history (3.4), (7.1) reduces to

$$U^2 = \frac{1}{\rho_R}\left(\frac{d\sigma_I(\varepsilon)}{d\varepsilon}\right) = \frac{1}{\rho_R}E_I(\varepsilon). \tag{7.2}$$

Considering the equilibrium strain history and using the specific form for $\hat{G}(\varepsilon; s)$ employed in the steady wave analysis (5.7), it is easily shown that the velocity of an acceleration wave propagating into a region which is in equilibrium is given by

$$U^2 = \frac{1}{\rho_R}\left\{\frac{d\sigma_E(\varepsilon)}{d\varepsilon} + \frac{2(1-\varepsilon)}{(2-\varepsilon)\varepsilon}[\sigma_I(\varepsilon)-\sigma_E(\varepsilon)]\right\}. \tag{7.3}$$

Further, if the region is unstrained and at rest both (7.2) and (7.3) reduce to $U_0 = (C_I)_0$.

Using the representations for σ_E and σ_I in terms of strain developed in Section 5.2 and (2.9), one may easily calculate the acceleration wave velocities predicted by (7.2) and (7.3). The curves shown in Fig. 10 labeled I and E are the results of such calculations. It is seen that the velocity corresponding to the jump history, curve I, is always greater than the velocity corresponding to the equilibrium history, curve E.

The unloading wave velocities shown in Table 1 are average velocities calculated from $U = (X_m + X_p)[t_a - X_p/U_s]^{-1}$ where X_m is the mirror location, X_p is the thickness of the flyer, t_a the time after impact at which the unloading wave arrives, and U_s is the measured shock velocity. For a given impact condition, no significant variation of unloading wave velocity was observed over the range of propagation distances (typically from 6 to 42 mm). The measured unloading wave velocity and corresponding equilibrium strain values are plotted in Fig. 10. It is seen that for strains less than about 6 per cent good agreement

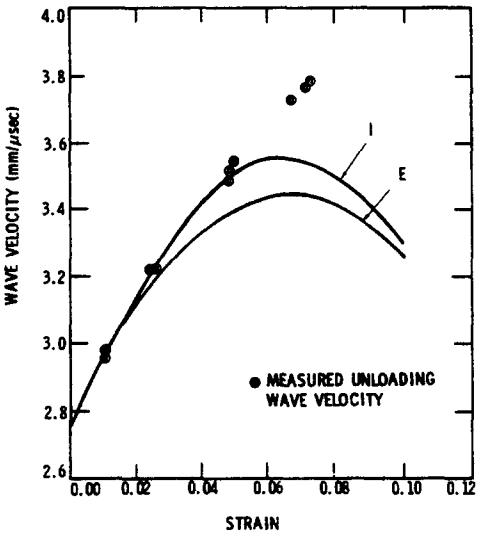

FIG. 10. Comparison of observed and calculated acceleration wave speeds.

exists between the calculated velocity corresponding to the jump history, curve I, and the observed unloading wave velocity. The velocity corresponding to the equilibrium history tends to fall below the experimental points. The lack of agreement above about 6 per cent strain (7·5 kbar) is indicative of the inflection in the equilibrium behavior of PMMA reported by Schuler [32] and Barker and Hollenbach [24] and due to the fact that the existence of a steady wave in PMMA traveling faster than 3·1 mm/μsec is not consistent with the constitutive assumption of finite linear viscoelasticity.

Nevertheless, this study of unloading waves suggests an alternative method of formulating a constitutive model. The weak dependence of acceleration wave velocity on strain history suggests assuming that the wave speed is a function of the current value of strain alone, namely that given by (7·2). With this assumption, measurements of unloading wave speed then determine the instantaneous stress–strain curve. Over the 0–7·5 kbar range the instantaneous curve determined in this manner differs little from that determined by the methods outlined in Section 5. At higher stress levels this assumption leads to a nonlinear Maxwellian constitutive model which has been successfully used by Schuler and Nunziato [33] to describe the behavior of PMMA to 60 kbar.

7.2 *The growth of acceleration waves*

As shown in Section 3.2, the growth or decay of an acceleration wave propagating into an unstrained region at rest is governed by a critical amplitude a_c and a constant β, both of which depend upon the acceleration wave velocity U_0, the instantaneous tangent modulus $(E_I)_0$, the instantaneous second-order modulus $(\tilde{E}_I)_0$, and the initial slope of the stress relaxation function $G_0'(0)$. Methods for determining these constants from the results of steady shock wave experiments have been suggested by Walsh and Schuler [12] and by Chen and Gurtin [39].

The quantities $(E_I)_0$ and $(\tilde{E}_I)_0$ are determined directly from the instantaneous stress–strain curve $\sigma_I(\varepsilon)$ by using $(3.11)_{1,2}$. The velocity U_0 can be computed by $\rho_R U_0^2 = (E_I)_0$ and, as we have already indicated, represents the lead coefficient of the steady shock

velocity–particle velocity fit (5.1), i.e., $U_0 = (C_I)_0$. In terms of these coefficients, $(\tilde{E}_I)_0 = 4\rho_R(C_I)_0^2 b_I$.

The final constant requiring evaluation is $G_0'(0)$, the initial slope of the stress relaxation function corresponding to the equilibrium strain history $\varepsilon^t(s) \equiv 0$. Chen and Gurtin [39] have observed that $G_0'(0)$ can be determined directly from experimental steady wave data as follows. In a steady shock wave, $(\dot{v})^- = U^2|\hat{\lambda}|$ (the critical acceleration). As shown in Section 6.1, this quantity can be evaluated graphically from steady wave profiles for various amplitudes v^-. Then, extrapolating this data to $v^- = 0$ and using $(3.23)_2$ yields the critical amplitude a_c. Finally, $G_0'(0)$ can be calculated by $(3.13)_2$. Although this approach is satisfactory in principle, the limited number of experimentally determined particle accelerations $(\dot{v})^-$ and their large uncertainty make the value obtained by an extrapolation to zero particle velocity very questionable (e.g., Fig. 7). Walsh and Schuler [12] have used an alternate technique to evaluate $G_0'(0)$ which in essence makes use of more experimental data. They evaluated (6.3), which is based on the constitutive model of finite linear viscoelasticity, at $\varepsilon = 0$ to obtain

$$G_0'(0) = -\frac{\rho_R}{\tau}[(C_I)_0^2 - (C_E)_0^2].$$

With these results, β and a_c can be calculated using (3.13) and then the critical time t_∞ as a function of the initial amplitude $a(0)$ is given by (3.15). This result, again for the polymer PMMA,† is shown in Fig. 11. Also shown in this figure is the $t_\infty(a(0))$ behavior for an elastic material‡ which has the same values for the tangent and second-order moduli as PMMA (curve labeled elastic).

Walsh and Schuler [12] also compared the predictions of Fig. 11 with experimental observations of the growth of acceleration waves in PMMA. The experimental configuration used is shown in Fig. 2(b). The generation of the acceleration wave is due to the unique properties of fused silica [24]. Unlike most materials the one-dimensional stress–strain curve of this elastic material (for stresses less than about 35 kbar) has a curvature such that compressive discontinuities tend to spread, i.e. $\tilde{E} < 0$. Thus, as the shock discontinuity produced at the impact surface propagates into the fused silica, it spreads continuously, forming an acceleration wave which is introduced into the PMMA. The amplitude of the acceleration discontinuity introduced varies inversely with the thickness of the fused silica. In order to maintain a one-dimensional motion for the duration of the experiment the thickness of the fused silica is limited to about 4 cm. This corresponds to a lower limit on the acceleration discontinuity producible with this technique of approximately 0·27 mm/μsec^2. Unfortunately, this value of $a(0)$ is greater than the value of a_c calculated above§ and thus, as expected, only acceleration waves which grow were observed.

The data from six experiments were available for correlation with the predicted behavior of acceleration waves in PMMA. These data which are shown in Fig. 12 (curves

† For PMMA, $U_0 = 2{\cdot}76$ mm/μsec, $(E_I)_0 = 90{\cdot}3$ kbar, $(\tilde{E}_I)_0 = 1312$ kbar, and $G_0'(0) = -6{\cdot}26$ kbar/μsec. Because of the possible hazards of twice differentiating an experimental data-fit function, the value of $(\tilde{E}_I)_0$ can be obtained in an alternate manner. A representation for $E_I(\varepsilon) = \rho_R U^2(\varepsilon)$ can be found directly from experimental measurements of acceleration wave velocities (unloading wave velocities) in prestrained material. Fitting the data discussed in Section 7.1 yields an alternate value of $(\tilde{E}_I)_0 = 1190$ kbar which is in good agreement. Cf. Walsh and Schuler [12].

‡ Cf. Thomas [40].

§ For PMMA, $a_c = 0{\cdot}0132$ mm/μsec^2.

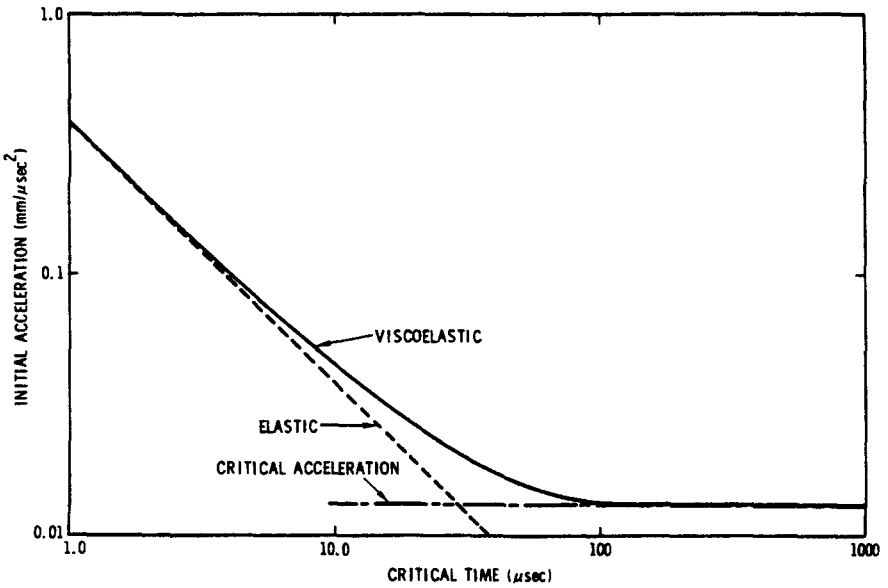

FIG. 11. Critical time vs initial acceleration wave amplitude.

A1, A2, A3 and B1, B2, B3)† can be grouped into two series depending on the thickness of the fused silica employed.

The first series (input A) employed a 25·5 mm thick piece of fused silica to obtain an initial acceleration wave amplitude of $0{\cdot}41 \pm 0{\cdot}01$ mm/μsec^2. From Fig. 11 this input wave amplitude corresponds to a critical time $t_\infty = 0{\cdot}94 \pm 0{\cdot}04$ μsec. The transit time from the interface to the mirror was 1·06, 1·63 and 2·25 μsec for shots A1, A2, A3, respectively.‡ Thus, in each of these experiments a shock discontinuity is expected to have

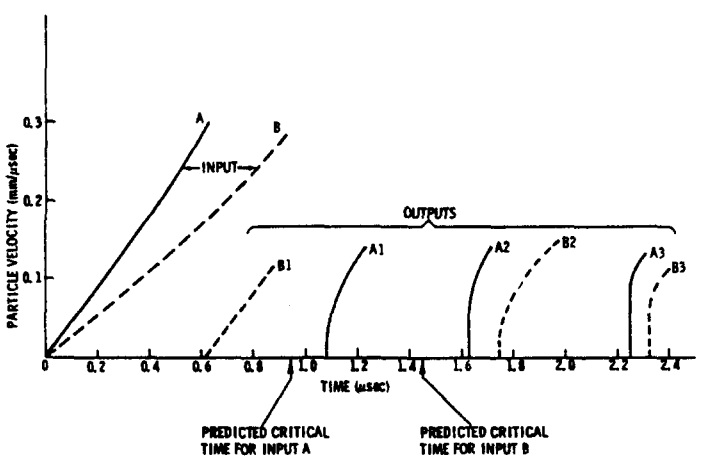

FIG. 12. Observed acceleration wave profiles.

† Two of these experiments (A3 and B3) were performed by Barker and Hollenbach [24]. The remainder are due to Walsh and Schuler [12].

‡ Here transit times are calculated from $t = X_m/U_0$.

formed. The wave profiles measured at the mirror are shown in Fig. 12 where it is clear that the shocks have formed.

The second series (input B) used a 38·1 mm thick piece of fused silica which yields an initial acceleration level of $a(0) = 0{\cdot}27 \pm 0{\cdot}01$ mm/μsec^2. From Fig. 11 the corresponding critical time is $t_\infty = 1{\cdot}45 \pm 0{\cdot}07$ μsec. Two of the shots in this series (B2, B3) had propagation times (1·74, 2·32 μsec, respectively) greater than t_∞. Thus, again, for B2, B3 a shock wave is expected to form and this is borne out in Fig. 12. In shot B1 a wave was observed after propagating for 0·63 μsec. Since this time is less than t_∞, the formation of the shock discontinuity is not predicted. The results are shown in Fig. 12 where, as predicted, no shock is evident. In addition, since $a(0) > a_c$, the acceleration amplitude is increasing and can be predicted from equation (3.14). Considering $a(0) = 0{\cdot}27 \pm 0{\cdot}01$ mm/μsec, we calculate $a(0{\cdot}63) = 0{\cdot}47 \pm 0{\cdot}03$ mm/μsec^2. The measured level of $0{\cdot}46 \pm 0{\cdot}02$ mm/μsec is in good agreement with this predicted value.

It is interesting to note from Fig. 11 that, at these levels of initial acceleration, the predicted t_∞ for PMMA is close to that for a nonlinear elastic solid with the same tangent and second-order moduli, E and $\tilde{E}$. Of course for elastic materials there is no critical acceleration. Nevertheless, an acceleration wave, whose initial amplitude is an order of magnitude greater than the critical acceleration, will propagate in nonlinear polymeric solids (such as PMMA) as if the material were elastic.† This observation suggests that in certain cases, the simpler elastic theory can be used to interpret the results of acceleration wave experiments conducted on nonlinear viscoelastic materials.

8. THERMODYNAMIC INFLUENCES ON VISCOELASTIC WAVE PROPAGATION

Up to this point we have considered the propagation of shock and acceleration waves in nonlinear viscoelastic materials neglecting thermal influences. The remainder of this article deals with such effects. In particular, following a short review of the thermodynamics of nonconducting materials with memory, a particular constitutive form for a thermoviscoelastic material is introduced and applied both to the steady shock wave problem and the growth and decay of shock waves. It is interesting to note that thermal effects have no influence on the propagation of acceleration waves in a nonconductor of heat. That is, if the relaxation function and second-order modulus are taken at fixed entropy, then the velocity of every acceleration wave satisfies (3.10) and the amplitude of an acceleration wave entering a region at rest, unstrained, and at uniform temperature, satisfies (3.12) and (3.13).‡ Thus, if the assumption that the material is a thermal nonconductor is valid (which seems reasonable for polymeric solids) the study of acceleration waves provides no information about the thermodynamic effects on the material response.

8.1 *Thermodynamics of materials with memory*§

A material with memory which does not conduct heat can be characterized by the following general constitutive assumption:

† By considering the asymptotic behavior of the solutions of the differential equation which governs acceleration wave propagation (Bernoulli's equation), Bailey and Chen [8] reach a similar conclusion.

‡ Cf. Coleman and Gurtin [41].

§ A comprehensive review of the thermodynamics of materials with fading memory has been given by Day [42].

(i) at a given material particle the free energy ψ at time t is determined by the entire past history of the strain ε^t and the temperature θ^t; i.e.†

$$\psi(t) = \mathscr{P}(\varepsilon^t, \theta^t) \tag{8.1}$$

where $\varepsilon^t(s) = \varepsilon(t-s)$, $\theta^t(s) = \theta(t-s)$, $0 \leq s < \infty$; and

(ii) the material exhibits "fading memory".

The concept of fading memory has been extended to functionals of the type (8.1) by Coleman [43] and by Mizel and Wang [44] and, in essence, implies that the functional $\mathscr{P}$ is three-times continuously differentiable on the space of all histories with finite norm (cf. (3.2)). Using this smoothness assumption and the second law (2.5), Coleman [43] has shown that the stress and the entropy are given by

$$\sigma(t) = \mathscr{L}(\varepsilon^t, \theta^t) = \partial_\varepsilon \mathscr{P}(\varepsilon^t, \theta^t), \tag{8.2}$$

$$\eta(t) = \mathscr{N}(\varepsilon^t, \theta^t) = -\partial_\theta \mathscr{P}(\varepsilon^t, \theta^t). \tag{8.3}$$

The internal energy is then calculated by

$$\mathrm{e}(t) = \mathscr{E}(\varepsilon^t, \theta^t) = \psi(t) + \theta(t)\eta(t). \tag{8.4}$$

Coleman has further shown that the free energy is a minimum when evaluated for the equilibrium histories $\varepsilon_E(s) = \varepsilon(t)$, $\theta_E(s) = \theta(t)$, $0 \leq s < \infty$. Then, defining

$$\omega_E(\varepsilon, \theta) = \mathscr{W}(\varepsilon_E, \theta_E)$$

as an *equilibrium response function* ($\omega = \psi$, σ, η, or e), the second law asserts that

$$\mathscr{P}(\varepsilon^t, \theta^t) \geq \psi_E(\varepsilon, \theta). \tag{8.5}$$

The assumed smoothness of the free energy functional $\mathscr{P}$ also insures that for small relative strain and temperature histories, γ^t, ϕ^t, the material response can be approximated by linear viscoelasticity, i.e.,

$$\begin{aligned}\mathscr{L}(\varepsilon^t + \gamma^t, \theta^t + \phi^t) = {} & \mathscr{L}(\varepsilon^t, \theta^t) + F_t(0)\gamma^t(0) + L_t(0)\phi^t(0) \\ & + \int_0^\infty F_t'(s)\gamma^t(s)\,\mathrm{d}s + \int_0^\infty L_t'(s)\phi^t(s)\,\mathrm{d}s + o(\|\gamma^t\| + \|\phi^t\|)\end{aligned} \tag{8.6}$$

as $\|\gamma^t\| + \|\phi^t\| \to 0$. The quantities $F_t(s)$ and $L_t(s)$ are called the *stress–strain relaxation function* and the *stress–temperature relaxation function*, respectively. An analogous approximation holds for $\mathscr{E}(\varepsilon^t + \gamma^t, \theta^t + \phi^t)$ which involves an *energy–strain relaxation function* $H_t(s)$ and an *energy–temperature relaxation function* $J_t(s)$. Again we have used the subscript t as a reminder that all these functions depend, in general, on the underlying histories ε^t, θ^t.

To evaluate the instantaneous response of the material, we consider the jump history

$$(\varepsilon_I(s), \theta_I(s)) = \begin{cases}(\varepsilon, \theta), & s = 0 \\ (0, \theta_0), & s > 0\end{cases} \tag{8.7}$$

with θ_0 the reference temperature corresponding to the unstrained state. Then,

$$\omega_I(\varepsilon, \theta) = \mathscr{W}(\varepsilon_I, \theta_I)$$

† The temperature is taken as the independent thermodynamic variable since it is amenable to direct measurement and is convenient for situations involving temperature-dependent thermophysical properties.

is an *instantaneous response function* ($\omega = \psi, \sigma, \eta$, or e). The relaxation functions corresponding to the jump history (8.7) are denoted as $F(\varepsilon, \theta; s)$, $L(\varepsilon, \theta; s)$, $H(\varepsilon, \theta; s)$ and $J(\varepsilon, \theta; s)$. Since ψ_I is of class C^3, σ_I and e_I are of class C^2 and it follows that

$$\begin{aligned} (E_T)_I &= \partial_\varepsilon \sigma_I(\varepsilon, \theta) = F(\varepsilon, \theta; 0), \\ A_I &= \partial_\theta \sigma_I(\varepsilon, \theta) = L(\varepsilon, \theta; 0), \\ \varkappa_I &= \partial_\theta e_I(\varepsilon, \theta) = J(\varepsilon, \theta; 0), \end{aligned} \tag{8.8}$$

which are called the *instantaneous isothermal tangent modulus*, *instantaneous stress–temperature modulus* and *instantaneous specific heat*, respectively. It will be useful in what follows to also define the *instantaneous stress–energy modulus* (Grüneisen parameter)

$$\Gamma_I = \frac{A_I}{\varkappa_I}. \tag{8.9}$$

We assume, as is natural, that

$$(E_T)_I > 0, \qquad A_I \neq 0, \qquad \varkappa_I > 0. \tag{8.10}$$

In terms of $(E_T)_I$, the *instantaneous isentropic tangent modulus* $(E_N)_I$ is given by†

$$(E_N)_I = (E_T)_I + \frac{\theta A_I^2}{\varkappa_I} > 0. \tag{8.11}$$

This modulus represents the slope of the instantaneous isentropic stress–strain curve $\sigma_I(\varepsilon, \eta)$; and hereafter, we assume that this curve is strictly convex from below.‡ Thus,

$$(E_N)_I = \partial_\varepsilon \sigma_I(\varepsilon, \eta) > 0, \qquad (\tilde{E}_N)_I = \partial_\varepsilon^2 \sigma_I(\varepsilon, \eta) > 0. \tag{8.12}$$

In a manner analogous to (8.8), (8.9), (8.11) and (8.12), we can define equilibrium moduli in terms of the equilibrium response functions and we assume that the equilibrium counterparts of the inequalities (8.10)–(8.12) hold. Coleman [45] and Coleman and Gurtin [46] have shown that the minimal property of the free energy functional requires that

$$((E_T)_I)_0 \geq ((E_T)_E)_0, \qquad (\varkappa_I)_0 \leq (\varkappa_E)_0 \tag{8.13}$$

where $(\cdot)_0$ denotes evaluation at the equilibrium state $(0, \theta_0)$.

8.2 *Steady shock waves*

While a proof of the existence of steady shock waves in general nonlinear thermoviscoelastic materials is lacking, such steady wave solutions have been exhibited by Nunziato and Walsh [47] who used a specific form for the free energy functional $\mathscr{P}$ to analyze the steady wave profiles experimentally observed by Schuler [25] in PMMA. As would be expected the overall properties of steady waves in the thermoviscoelastic case are qualitatively the same as in the purely mechanical case.

Constitutive model. Here we follow the study of Nunziato and Walsh [47] and introduce a specific thermoviscoelastic constitutive model. Motivated by the minimal property, the functional $\mathscr{P}$ is assumed to be the following quadratic form:

$$\psi(t) = \psi_E(\varepsilon, \theta) + \tfrac{1}{2} K(\varepsilon) \{\mathscr{J}(\varepsilon^t) + \mathscr{T}(\theta^t)\}^2 \tag{8.14}$$

† Cf. Coleman and Gurtin [41], (8.18).

‡ The existence of the curve $\sigma_I(\varepsilon, \eta)$ is assured by the fact that $\varkappa_I > 0$.

where $K(\varepsilon) > 0$ for all ε on (0, 1) and the functionals $\mathscr{J}(\varepsilon^t)$ and $\mathscr{T}(\theta^t)$ have the representations

$$\mathscr{J}(\varepsilon^t) = \varepsilon + \int_0^\infty f'(s)\varepsilon^t(s)\,ds, \tag{8.15}$$

$$\mathscr{T}(\theta^t) = -\frac{1}{\theta_0}\left[g_0\theta + \int_0^\infty g'(s)\theta^t(s)\,ds\right]. \tag{8.16}$$

Here $f(s)$ and $g(s)$ are the mechanical and thermal relaxation functions with the properties $f(0) = 1$, $g(0) = g_0 > 0$ and $f(s)$ and $g(s) \to 0$ as $s \to \infty$. The specific constitutive equations for the stress and the internal energy can be computed from (8.14) using (8.2)–(8.4):

$$\sigma(t) = \sigma_E(\varepsilon, \theta) + \tfrac{1}{2}K'(\varepsilon)\{\mathscr{J}(\varepsilon^t) + \mathscr{T}(\theta^t)\}^2 + K(\varepsilon)\{\mathscr{J}(\varepsilon^t) + \mathscr{T}(\theta^t)\}, \tag{8.17}$$

$$e(t) = e_E(\varepsilon, \theta) + \tfrac{1}{2}K(\varepsilon)\{\mathscr{J}(\varepsilon^t) + \mathscr{T}(\theta^t)\}^2 + K(\varepsilon)g_0\frac{\theta}{\theta_0}\{\mathscr{J}(\varepsilon^t) + \mathscr{T}(\theta^t)\}. \tag{8.18}$$

Evaluating (8.17) and (8.18) for the jump history (8.7) we obtain the relations

$$\sigma_I(\varepsilon, \theta) = \sigma_E(\varepsilon, \theta) + \tfrac{1}{2}K'(\varepsilon)h^2(\varepsilon, \theta) + K(\varepsilon)h(\varepsilon, \theta), \tag{8.19}$$

$$e_I(\varepsilon, \theta) = e_E(\varepsilon, \theta) + \tfrac{1}{2}K(\varepsilon)h(\varepsilon, \theta)\left[h(\varepsilon, \theta) + 2g_0\frac{\theta}{\theta_0}\right], \tag{8.20}$$

with $h(\varepsilon, \theta) = \varepsilon - g_0(\theta/\theta_0 - 1)$. Hereafter, we assume that $(0, \theta_0)$ corresponds to a *natural* equilibrium state of the material and thus,

$$(\sigma_I)_0 = (\sigma_E)_0 \equiv 0, \qquad (e_I)_0 = (e_E)_0 \equiv e_0.$$

It is interesting to note that for this particular model, with $g_0 > 0$,

$$(A_I)_0 \leq (A_E)_0. \tag{8.21}$$

This inequality has been found to hold for PMMA by Nunziato and Walsh [48] and it is expected on physical grounds to hold for most polymers. This observation along with (8.13) suggests that the instantaneous and equilibrium surfaces in stress–strain–temperature space intersect and Fig. 13 is an illustration of this. It is clear from (8.19) that the projection of the line of intersection is given in the temperature–strain plane by $h(\varepsilon, \theta) = 0$.

Steady shock waves. In considering steady motions in thermoviscoelastic media, the temperature is also assumed to be steady:

$$\theta(X, t) = \theta(\xi), \qquad \xi = t - \frac{X}{V}.$$

The corresponding particle velocity and strain fields are given by (3.25). Steady strain and temperature fields imply the existence of steady stress and internal energy fields through (8.17) and (8.18). Thus, for natural equilibrium conditions ($\varepsilon = 0$, $\theta = \theta_0$, $\sigma = 0$, $e = e_0$) far ahead of the wave, the balance equations of momentum (2.3) and energy (2.4) reduce to

$$\sigma(\xi) = \rho_R V^2 \varepsilon(\xi), \tag{8.22}$$

$$e(\xi) = e_0 + \tfrac{1}{2}\rho_R V^2 \varepsilon^2(\xi) = e_0 + \tfrac{1}{2}\sigma(\xi)\varepsilon(\xi) \tag{8.23}$$

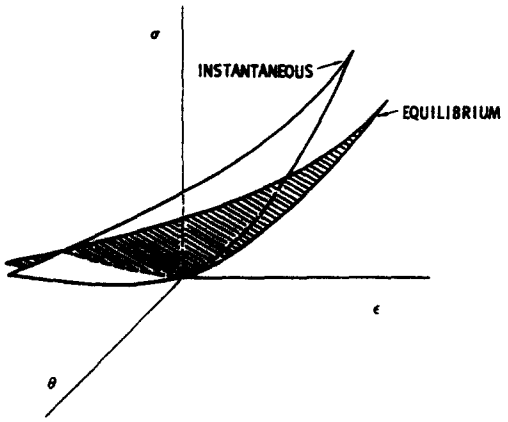

FIG. 13. Instantaneous and equilibrium stress–strain–temperature surfaces.

for all values of ξ. These relations combine with the constitutive equations (8.17) and (8.18) to yield a coupled set of integral equations for the steady strain and temperature fields $\varepsilon(\xi)$ and $\theta(\xi)$:

$$\begin{aligned}\rho_R V^2 \varepsilon(\xi) &= \sigma_E(\varepsilon(\xi), \theta(\xi)) + \tfrac{1}{2}K'(\varepsilon(\xi))\{\mathscr{J}(\varepsilon(\xi-s)) + \mathscr{T}(\theta(\xi-s))\}^2 \\ &\quad + K(\varepsilon(\xi))\{\mathscr{J}(\varepsilon(\xi-s)) + \mathscr{T}(\theta(\xi-s))\}, \\ e_0 + \tfrac{1}{2}\rho_R V^2 \varepsilon^2(\xi) &= e_E(\varepsilon(\xi), \theta(\xi)) + \tfrac{1}{2}K(\varepsilon(\xi))\{\mathscr{J}(\varepsilon(\xi-s)) + \mathscr{T}(\theta(\xi-s))\}^2 \\ &\quad + K(\varepsilon(\xi))g_0 \frac{\theta(\xi)}{\theta_0}\{\mathscr{J}(\varepsilon(\xi-s)) + \mathscr{T}(\theta(\xi-s))\}.\end{aligned} \tag{8.24}$$

Here we will confine our attention to steady shock wave solutions, i.e. solutions for given values of the steady wave velocity V with

$$V^2 > (C_I)_0^2 = \frac{((E_N)_I)_0}{\rho_R} \tag{8.25}$$

where, as before, $(C_I)_0$ is the instantaneous longitudinal sound speed corresponding to the equilibrium reference state. Such solutions of (8.24) can satisfy the equilibrium conditions far ahead of the wave only if $\varepsilon(\xi) = 0$, $\theta(\xi) = \theta_0$ for $\xi < 0$ and there is a jump discontinuity in strain ε and temperature θ at $\xi = 0$. However, to proceed further and obtain steady shock solutions, the material functions involved in (8.24) must be determined; namely, the equilibrium functions $\sigma_E(\varepsilon, \theta)$, $e_E(\varepsilon, \theta)$, the function $K(\varepsilon)$, and the relaxation functions $f(s)$ and $g(s)$. A procedure for evaluating these response functions from experimental steady shock wave, thermophysical, and bulk response data has been developed by Nunziato and Walsh [47] and applied to the solid polymer, PMMA.

Determination of response functions. As we have already seen in Section 5, measurements of the steady wave velocity V and the particle velocity v at the head and the tail of a steady shock wave enables one to determine the instantaneous and equilibrium response functions, $\sigma_I(\varepsilon)$ and $\sigma_E(\varepsilon)$. In the present context, these functions represent the *instantaneous* and *equilibrium Hugoniot stress–strain curves* for the material and can be represented in

terms of least-squares polynomial fits in strain,

$$\begin{aligned}\sigma_I(\varepsilon) &= l_I\varepsilon + m_I\varepsilon^2 + n_I\varepsilon^3,\\ \sigma_E(\varepsilon) &= l_E\varepsilon + m_E\varepsilon^2 + n_E\varepsilon^3,\end{aligned} \tag{8.26}$$

with the coefficients corresponding to the equilibrium state $(0, \theta_0)$ ahead of the wave.† In Schuler's [25] experiments, $\theta_0 = 295°\text{K}$. The coefficients l_I and l_E are related to the instantaneous and equilibrium sound speeds by‡

$$l_I = \rho_R(C_I)_0^2, \qquad l_E = \rho_R(C_E)_0^2. \tag{8.27}$$

Since the energy equation (8.23) must hold everywhere in a steady wave, evaluation of this expression at the shock front and at the tail of the wave yields

$$\begin{aligned}H_I(\varepsilon, \theta) &= \mathrm{e}_I(\varepsilon, \theta) - \mathrm{e}_0 - \tfrac{1}{2}\sigma_I(\varepsilon, \theta)\varepsilon = 0,\\ H_E(\varepsilon, \theta) &= \mathrm{e}_E(\varepsilon, \theta) - \mathrm{e}_0 - \tfrac{1}{2}\sigma_E(\varepsilon, \theta)\varepsilon = 0.\end{aligned} \tag{8.28}$$

The functions $H_I(\cdot, \cdot)$ and $H_E(\cdot, \cdot)$ are called the *instantaneous and equilibrium Hugoniot temperature–strain curves.* Since the Hugoniot stress–strain curves (8.26) are one-to-one, the Hugoniot temperature–strain curves must also be one-to-one,§ and we assume they have the representations

$$\begin{aligned}\Theta_I(\varepsilon) &= \theta_0\{1 + \tilde{a}_I\varepsilon + \tilde{b}_I\varepsilon^2\},\\ \Theta_E(\varepsilon) &= \theta_0\{1 + \tilde{a}_E\varepsilon + \tilde{b}_E\varepsilon^2\}.\end{aligned} \tag{8.29}$$

The coefficients $\tilde{a}_I$, $\tilde{b}_I$, $\tilde{a}_E$, $\tilde{b}_E$ also depend upon the reference state $(0, \theta_0)$ and, after some lengthy calculations, can be evaluated from thermophysical data.‖ The Hugoniot temperature-strain curves for PMMA are shown in Fig. 14.

The material function $K(\varepsilon)$ is evaluated using (8.20) and steady shock wave data:

$$K(\varepsilon) = \frac{2\{\mathrm{e}_I(\varepsilon) - \mathrm{e}_E(\varepsilon, \Theta_I(\varepsilon))\}}{h(\varepsilon, \Theta_I(\varepsilon))\left\{h(\varepsilon, \Theta_I(\varepsilon)) + 2g_0\dfrac{\Theta_I(\varepsilon)}{\theta_0}\right\}} \tag{8.30}$$

where $\mathrm{e}_I(\varepsilon) = \mathrm{e}_I(\varepsilon, \Theta_I(\varepsilon)) = \mathrm{e}_0 + \frac{1}{2}\sigma_I(\varepsilon)\varepsilon$ and the constant g_0, which is a measure of the thermal relaxation, is also calculated from thermophysical data.

The form for the equilibrium response functions, $\sigma_E(\varepsilon, \theta)$ and $\mathrm{e}_E(\varepsilon, \theta)$ is based upon an explicit assumption for the equilibrium internal energy function:

$$\mathrm{e}_E(\varepsilon, \theta) = \mathrm{e}_0 + \int_{\theta_0}^{\theta} \varkappa_E(0, \omega)\,\mathrm{d}\omega + D(\varepsilon)W(\theta), \tag{8.31}$$

† For PMMA, the values of the coefficients are: $l_I = 90{\cdot}43$ kbar, $m_I = 681{\cdot}1$ kbar, $n_I = -1396$ kbar, $l_E = 39{\cdot}37$ kbar, $m_E = 680{\cdot}7$ kbar, $n_E = -2720$ kbar. The curves are shown in Fig. 5(b).

‡ In the present case, $(C_I)_0 = 2{\cdot}76$ mm/μsec, $(C_E)_0 = 2{\cdot}73$ mm/μsec. The difference in the value of $(C_E)_0$ given here and that value given previously is due to the way the experimental data were fitted.

§ Cf. Nunziato and Herrmann [49].

‖ Cf. Nunziato and Walsh [47]. For PMMA, the coefficients are: $\tilde{a}_E = (\Gamma_E)_0 = 0{\cdot}66$, $\tilde{b}_E = -1{\cdot}50$, $\tilde{a}_I = (\Gamma_I)_0 = 0{\cdot}55$, $\tilde{b}_I = -0{\cdot}94$.

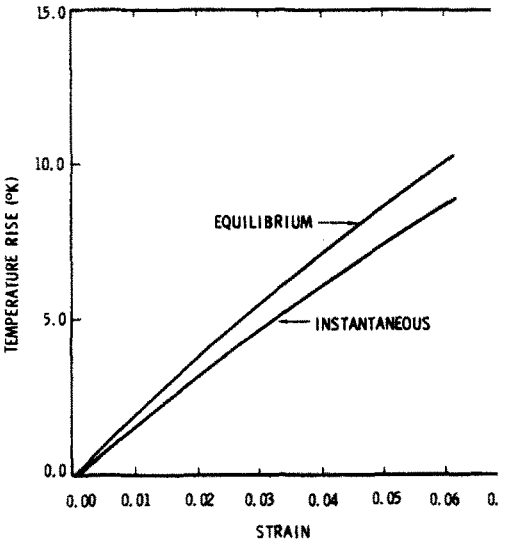

FIG. 14. Instantaneous and equilibrium Hugoniot temperature–strain curves.

where $D(0) = 0$, $W(\theta_0) = 1$. Then, using the equilibrium counterparts of (8.2)–(8.4) and (8.31), the equilibrium stress function is found to be given by

$$\sigma_E(\varepsilon, \theta) = M(\varepsilon)\frac{\theta}{\theta_0} - \theta D'(\varepsilon)\int_{\theta_0}^{\theta} \frac{W(\omega)}{\omega^2}\,\mathrm{d}\omega. \tag{8.32}$$

The strain-dependent functions $D(\varepsilon)$ and $M(\varepsilon)$ are evaluated from the results of steady wave experiments, i.e. using (8.31) and (8.32) along with $(8.29)_2$ and the fact that $\sigma_E(\varepsilon) = \sigma_E(\varepsilon, \Theta_E(\varepsilon))$:

$$L(\varepsilon) = \frac{1}{G(\Theta_E(\varepsilon))}\left\{\tfrac{1}{2}\sigma_E(\varepsilon)\varepsilon - \int_{\theta_0}^{\Theta_E(\varepsilon)} \varkappa_E(0, \omega)\,\mathrm{d}\omega\right\},$$

$$M(\varepsilon) = \frac{\theta_0}{\Theta_E(\varepsilon)}\left\{\sigma_E(\varepsilon) + \Theta_E(\varepsilon)L'(\varepsilon)\int_{\theta_0}^{\Theta_E(\varepsilon)} \frac{W(\omega)}{\omega^2}\,\mathrm{d}\omega\right\}.$$

It follows from (8.32) that

$$W(\theta) = 1 + \int_{\theta_0}^{\theta} \frac{\omega}{\theta_0 (A_E)_0}\partial_\theta A_E(0, \omega)\,\mathrm{d}\omega.$$

To evaluate the equilibrium response functions, we need, in addition to the steady shock wave data, the temperature dependence of the equilibrium stress–temperature modulus $A_E(0, \theta)$ and the equilibrium specific heat $\varkappa_E(0, \theta)$ at zero strain. For a particular viscoelastic material, the modulus $A_E(0, \theta)$ can be calculated from measured values of the equilibrium coefficient of linear thermal expansion β_E and the equilibrium isothermal bulk modulus B_E:†

$$A_E(0, \theta) = 3\beta_E(\theta)B_E(\theta). \tag{8.33}$$

† The instantaneous and equilibrium bulk response of nonlinear viscoelastic solids has been considered by Nunziato, Schuler and Walsh [50]. A more complete discussion of the bulk properties of polymers is contained in the review article by Curro [51].

Then, the function $\varkappa_E(0, \theta)$ is computed from the measured equilibrium specific heat at zero pressure $\tilde{\varkappa}_E$.

$$\varkappa_E(0, \theta) = \tilde{\varkappa}_E(\theta) - 3\theta A_E(0, \theta)\beta_E(\theta). \tag{8.34}$$

Using data for PMMA obtained by Touloukian [52] and Heydemann and Guicking [53], A_E and $\varkappa_E$ can be represented by†

$$\begin{aligned} A_E(0, \theta) &= A_0 + A_1\theta + A_2\theta^2 + A_3\theta^3, \\ \varkappa_E(0, \theta) &= \varkappa_0 + \varkappa_1\theta + \varkappa_2\theta^2 + \varkappa_3\theta^3. \end{aligned} \tag{8.35}$$

Finally, the calculation of steady shock wave solutions requires that the relaxation functions $f(s)$ and $g(s)$ be specified. Motivated by the successful use of an exponential relaxation function in the purely mechanical theory (cf. Section 5), it is assumed that

$$f(s) = \exp\left(\frac{-s}{\tau_\varepsilon}\right), \qquad g(s) = g_0 \exp\left(\frac{-s}{\tau_\theta}\right). \tag{8.36}$$

The mechanical relaxation time τ_ε to be used for PMMA will be that determined from acoustic dispersion data by Nunziato and Sutherland [30]; while the thermal relaxation time τ_θ will be evaluated by obtaining the best overall agreement between calculated and experimentally observed steady wave profiles. This completes the determination of the relevant material functions for the steady wave problem and, in essence, serves to completely characterize the dynamic thermoviscoelastic response of PMMA.

Steady shock wave solutions. Now, as was indicated previously, a steady shock wave involves a jump discontinuity in strain ε and temperature θ (and particle velocity v) at $\xi = 0$. The value $\varepsilon(0)$ is determined by (8.22) and (8.26); i.e., $\varepsilon(0)$ is the smallest positive root of the quadratic

$$n_I\varepsilon^2 + m_I\varepsilon + \rho_R[(C_I)_0^2 - V^2] = 0.$$

The maximum strain $\varepsilon(\infty)$ achieved for a given steady wave velocity V is the smallest positive root of

$$n_E\varepsilon^2 + m_E\varepsilon + \rho_R[(C_E)_0^2 - V^2] = 0.$$

The corresponding temperatures, $\theta(0) = \Theta_I(\varepsilon(0))$ and $\theta(\infty) = \Theta_E(\varepsilon(\infty))$, are calculated by (8.29).

To obtain steady shock wave solutions, Nunziato and Walsh [47] solved the coupled integral equations (8.24) numerically. In particular, (8.24) can be converted to a coupled set of ordinary differential equations which, with the material functions known, can be integrated for the strain $\varepsilon(\xi)$ and the temperature $\theta(\xi)$ by using a Runge–Kutta integration technique. The corresponding particle velocity profile $v(\xi)$ follows from $(3.25)_2$. In Fig. 15, the comparison between calculated steady wave profiles and wave profiles experimentally observed by Schuler [25] are shown for the impact conditions of 0·15 mm/μsec (upper profile) and 0·30 mm/μsec (lower profile). These are the same profiles considered for the mechanical case and again we see that good agreement is obtained by using slightly adjusted steady wave velocities of 2·963 and 3·106 mm/μsec, respectively. The thermal relaxation time providing the best agreement was $\tau_\theta = 0{\cdot}10$ μsec. It is of interest to point

† The values of the coefficients are: $A_0 = 0{\cdot}762 \times 10^{-2}$ kbar/°K, $A_1 = 0{\cdot}163 \times 10^{-4}$ kbar/°K^2, $A_2 = 1{\cdot}14 \times 10^{-8}$ kbar/°K^3, $A_3 = -0{\cdot}727 \times 10^{-10}$ kbar/°K^4, $\varkappa_0 = -0{\cdot}460 \times 10^{-2}$ kbar/°K, $\varkappa_1 = 1{\cdot}75 \times 10^{-4}$ kbar/°K^2, $\varkappa_2 = -0{\cdot}688 \times 10^{-6}$ kbar/°K^3, $\varkappa_3 = 0{\cdot}106 \times 10^{-8}$ kbar/°K^4.

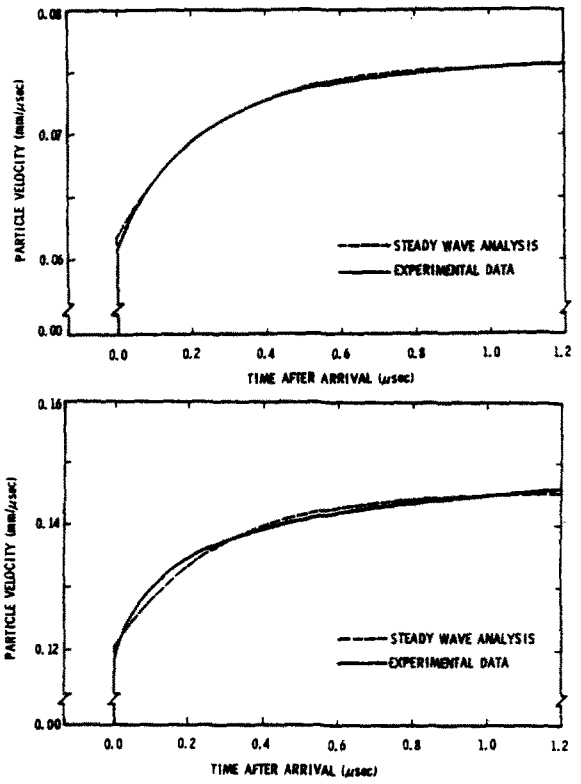

FIG. 15. Comparison of observed and calculated steady wave profiles.

out that the profiles are indeed sensitive to the relaxation time τ_θ. This may seem to be somewhat surprising since steady wave propagation is essentially a mechanical problem. As one would expect, the corresponding temperature profiles show the same overall structure as the particle velocity profiles.

Finally, it should be noted that due to the observed inflection in the equilibrium response of PMMA the thermoviscoelastic model constructed here is only expected to be valid for stresses up to approximately 7·5 kbars.

8.3 *Shock wave growth and decay*

Thermodynamic influences on the propagation of one-dimensional shock waves in nonconducting materials with memory have been considered by Coleman and Gurtin [54] and Chen and Gurtin [55].† Using a general constitutive assumption similar to (8.1), Chen and Gurtin [55] derived a differential equation analogous to (3.20) which relates the strain ε^- and the strain gradient $(\partial_X \varepsilon)^-$ behind the wave when the region ahead of the wave is in an unstrained equilibrium state. This shock amplitude equation serves to establish the existence of a critical strain gradient which governs the growth and decay of the wave. Here we outline Chen and Gurtin's [55] analysis and give some recent results obtained by Nunziato and Walsh [59] concerning a verification of the concept of the critical strain gradient for PMMA.

† Shock wave propagation in materials with memory which do conduct heat has been considered by Achenbach, Vogel and Herrmann [56, 57] and by Dunwoody [58].

Shock amplitude equation. In the presence of thermodynamic influences, the shock wave is assumed to be propagating into a region which is unstrained and at constant temperature for all past times; i.e., if $Y(t)$ is the location of the wave front, then, for $X > Y(t)$, $\varepsilon^t(s) \equiv 0$, $\theta^t(s) \equiv \theta_0$, $0 < s < \infty$. Across the shock, the temperature, as well as the strain, is discontinuous:

$$[\theta] = \theta^- - \theta_0, \qquad [\varepsilon] = \varepsilon^-.$$

Then, (2.9) to (2.12) represent the appropriate compatibility and balance equations at the wave and combine to give

$$\rho_R U^2 = \frac{[\sigma]}{[\varepsilon]}, \qquad [\mathrm{e}] = \tfrac{1}{2}(\sigma^- + \sigma^+)[\varepsilon]. \tag{8.37}$$

Equation $(8.37)_2$ is the well-known Hugoniot relation and along with (8.10) implies the existence of an instantaneous Hugoniot stress–strain curve defined by

$$\hat{H}_I(\varepsilon^-, \sigma^-) = \mathrm{e}_I(\varepsilon^-, \sigma^-) - \mathrm{e}_0 - \tfrac{1}{2}(\sigma^- + \sigma^+)\varepsilon^- = 0 \tag{8.38}$$

which represents the locus of stress–strain states $(\varepsilon^-, \sigma^-)$ attainable in a shock jump from the initial state $(0, 0)$. The Hugoniot curve is not closed and the relation between stress and strain on the curve need not be one-to-one. Nunziato and Herrmann [49] have considered the general properties of the curve (8.38) and, using the convexity of the instantaneous isentropic stress–strain law, established the following:†

(i) the shock is compressive; i.e. $\varepsilon^- > 0$,

(ii) the entropy η^- and the shock velocity U monotonically increase as the Hugoniot stress–strain curve is traversed outward from the origin $(0, 0)$, and

(iii) the shock velocity is subsonic with respect to the material behind the wave, i.e. $\rho_R U^2 < (E_N)_I^-$.

Under these conditions the following shock amplitude equation is obtained for the strain ε^- across the shock front:‡

$$\frac{\mathrm{d}\varepsilon^-}{\mathrm{d}t} = B\{\lambda - (\partial_X \varepsilon)^-\}, \tag{8.39}$$

where

$$B = \frac{2U\mu\alpha}{3\mu + \alpha(4 - 3\mu)}, \qquad \mu = 1 - \frac{\rho_R V^2}{(E_N)_I^-}, \qquad \alpha = \frac{2}{\varepsilon^- \Gamma_I^-} - 1. \tag{8.40}$$

As might be expected (in view of the results of Section 3.3), λ given by

$$\lambda = \frac{1}{\mu U (E_N)_I^-}\{F'(\varepsilon^-, \theta^-; 0)\varepsilon^- - L'(\varepsilon^-, \theta^-; 0)(\theta^- - \theta_0) - \Gamma_I^-[H'(\varepsilon^-, \theta^-; 0)\varepsilon^- - J'(\varepsilon^-, \theta^-; 0)(\theta^- - \theta_0)]\} \tag{8.41}$$

determines the growth or decay behavior of the wave and so is (again) called the *critical strain gradient.* We expect that for a reasonable range of strain levels $\lambda < 0$.§

† Coleman and Gurtin [54] established these same results by assuming that the instantaneous Hugoniot curve is one-to-one.

‡ Cf. Chen and Gurtin [55].

§ This is the case, for example, for PMMA, at least for $\varepsilon < 0{\cdot}04$.

Of course, before defining in detail the influence of λ on the wave amplitude, we must determine the sign of B. First of all it is clear from (iii) that $0 < \mu < 1$. Hence, since $U > 0$ it follows that the sign of B depends upon the sign of α, given by $(8.40)_3$. If it is now assumed, as is the case for most materials, that $\Gamma_I > 0$ and that the instantaneous Hugoniot stress–strain curve (8.38) is one-to-one, then $\alpha > 0$.† Thus, $B > 0$, and with $\lambda < 0$, it follows that

(i) if $\lambda < (\partial_X \varepsilon)^-$, $\dfrac{d\varepsilon^-}{dt} < 0$,

(ii) if $\lambda = (\partial_X \varepsilon)^-$, $\dfrac{d\varepsilon^-}{dt} = 0$, or

(iii) if $\lambda > (\partial_X \varepsilon)^-$, $\dfrac{d\varepsilon^-}{dt} > 0$.

Naturally, similar results can be given in terms of particle velocity v^- and the particle acceleration $(\dot{v})^-$ behind the shock front.

Determination of material functions. The procedure for determining the relaxation functions is similar to that followed in Section 6.1 for the mechanical model. That is, it is necessary to relate the response functions of the thermoviscoelastic model (8.14)–(8.16) to those defined in the more general formulation (8.1) in terms of which the results (8.39)–(8.41) are given. To do this we compute the derivatives of the stress, given by (8.17), and the internal energy, given by (8.18), with respect to the relative strain and temperature history and evaluate this for the appropriate underlying history. Carrying this out and evaluating the results for the jump history (8.7) yields the following identification between the relaxation functions:

$$\begin{aligned} F'(\varepsilon, \theta; 0) &= -\frac{1}{\tau_\varepsilon}[K'(\varepsilon)h(\varepsilon, \theta) + K(\varepsilon)], \\ L'(\varepsilon, \theta; 0) &= \frac{g_0}{\theta_0 \tau_\theta}[K'(\varepsilon)h(\varepsilon, \theta) + K(\varepsilon)], \\ H'(\varepsilon, \theta; 0) &= -\frac{K(\varepsilon)}{\tau_\varepsilon}(\varepsilon + g_0), \\ J'(\varepsilon, \theta; 0) &= \frac{g_0 K(\varepsilon)}{\theta_0 \tau_\theta}(\varepsilon + g_0). \end{aligned} \tag{8.42}$$

Here, as before, $h(\varepsilon, \theta) = \varepsilon - g_0(\theta/\theta_0 - 1)$, and τ_ε and τ_θ are the relaxation times.

The moduli $(E_N)_I$ and Γ_I can also be expressed in terms of the equilibrium functions and $K(\varepsilon)$. Evaluating the stress and energy relations (8.17) and (8.18) for the jump history (8.7) we can compute the instantaneous moduli (8.8):

$$\begin{aligned} (E_T)_I &= (E_T)_E + \tfrac{1}{2}K''(\varepsilon)h^2(\varepsilon, \theta) + 2K'(\varepsilon)h(\varepsilon, \theta) + K(\varepsilon), \\ A_I &= A_E - \frac{g_0}{\theta_0}[K'(\varepsilon)h(\varepsilon, \theta) + K(\varepsilon)], \\ \varkappa_I &= \varkappa_E - K(\varepsilon)g_0^2\frac{\theta}{\theta_0^2}. \end{aligned}$$

Combining these relations with (8.9) and (8.11) yields the desired results.

† See, e.g. Nunziato and Herrmann [49]. Chen and Gurtin [55] follow a similar argument.

It should be clear now that to complete the calculation of $\lambda(\varepsilon^-)$ we require the functions $\sigma_E(\varepsilon, \theta)$, $e_E(\varepsilon, \theta)$, $K(\varepsilon)$, $U(\varepsilon^-)$, $\theta^- = \Theta_I(\varepsilon^-)$, and the constants τ_ε, τ_θ and g_0. The method of determination of these quantities from data obtained by steady shock wave experiments and acoustic measurements, along with thermophysical properties, was given in the previous section.

Comparison with experimental results. Here we compare the values of the critical strain gradient $\lambda(\varepsilon^-)$ calculated by (8.41) with experimental studies, in particular, the steady shock wave studies using PMMA. As in Section 6.1, we give the results in terms of the critical acceleration $U^2|\lambda|$.† Since the waves were steady, the value of the particle acceleration behind the wave $(\dot{v})^-$ should be the critical acceleration. Figure 7 shows the comparison in terms of particle velocity. The solid line indicates the amplitude-dependence of $U^2|\lambda|$ using the constitutive model, results of steady wave experiments, and thermophysical data, as described above. The correlation between the measured values from the experimental studies and the calculated curve is reasonable.

The curve of $U^2|\lambda|$ is somewhat higher than the one for the mechanical model and partially indicates the influence of the thermodynamic effects on shock propagation in nonlinear polymeric materials.

In the limit of zero amplitude at the shock, Chen and Gurtin [55] have shown that in a nonconductor the value of the critical acceleration has a magnitude twice that of the critical amplitude of an acceleration wave. The value determined from the results discussed here predicts a critical time at which an acceleration wave will (appear to) form a shock discontinuity in PMMA which is consistent with the experimental observations presented in Section 7.2.

As mentioned earlier, since in general the time variation of the particle acceleration behind the wave is not known, it is not possible to determine $\varepsilon^-(t)$ completely from (8.40). Nevertheless, by making certain assumptions on $(\partial_X \varepsilon)^-$ it is possible to gain some insight into the amplitude behavior of a shock discontinuity which might be expected. In [59] Nunziato and Walsh assume $(\partial_X \varepsilon)^-$ to be constant at a value (i) greater than and (ii) less than λ and show the resulting growth and decay behavior of a wave.

8.4 *Stress–energy response*

Our entire discussion up to this point has dealt with one-dimensional wave propagation in nonlinear viscoelastic materials which can be produced by mechanical impact. However, in the context of thermoviscoelastic response it is also worthwhile to consider the one-dimensional response of the material to thermal impact, i.e., the response to rapid deposition of energy. Important factors in predicting such response are the instantaneous and equilibrium stress–energy curves at zero strain. Using the thermoviscoelastic model constructed in Section 8.2, Nunziato and Walsh [48] have calculated the stress–energy curves for PMMA and their results are shown in Fig. 16. Also shown here is the experimental result obtained by Barker‡ for a PMMA sample which essentially involved an instantaneous deposition of energy corresponding to a significant temperature rise. The good agreement with the instantaneous curve gives further support to the usefulness of the model constructed.

It is interesting to note that, unlike the mechanical stress–strain response (Fig. 5b), the instantaneous stress-energy response is *less* than the equilibrium response. This appears

† Cf. Section 3.3.

‡ L. M. Barker, private communication (1972).

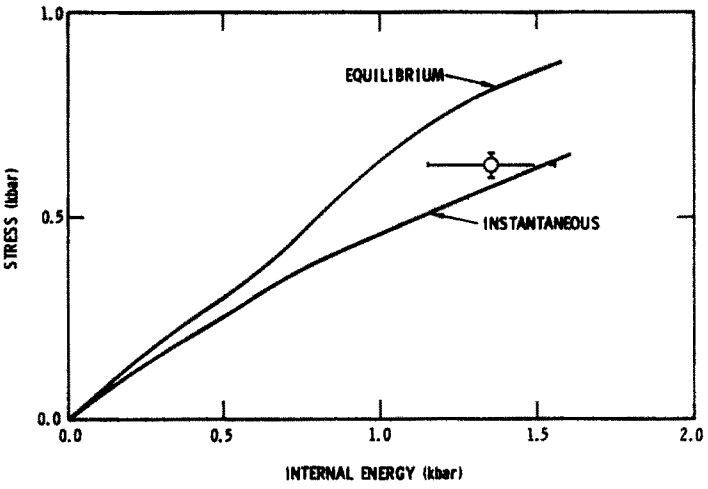

FIG. 16. Instantaneous and equilibrium stress–energy curves.

to be due to the manner in which energy is absorbed and transferred in a polymer. In the case of rapid energy deposition, the energy is initially absorbed by the high frequency modes and then is transferred over a period of tens of nanoseconds to the translational modes. Since it is the translational modes which contribute to the stress, the stress increases with time in a constant volume situation. It is for this reason that, as we observed previously, $(A_I)_0 \leq (A_E)_0$.

9. CLOSURE

In this article we have attempted to give a review of recent results concerning the propagation of one-dimensional waves in nonlinear viscoelastic materials. In particular, the main results of studies involving both shock and acceleration wave propagation in general materials with memory have been summarized and it has been shown that these results correlate very well with experimental observations on the polymer, polymethyl methacrylate. Fundamental to this work is the existence of steady shock waves and the fact that they can be generated in a truly one-dimensional experimental configuration. From such experimental observations one can determine the relevant material response functions for predicting the wave propagation behavior of the material in other one-dimensional situations. Furthermore, using a suitable constitutive assumption (either purely mechanical or thermomechanical), the complete one-dimensional constitutive equation governing the material can be evaluated from these steady shock wave measurements.

It should be emphasized that the present discussion deals with only one aspect of nonlinear viscoelastic wave propagation. There are several other important aspects, in their early stages of development, which should also be mentioned. One concerns obtaining complete solutions to the initial-boundary-value problems associated with the generation and subsequent propagation of shock and acceleration waves. Work in this area involves the use of numerical techniques and, in this connection, the viscoelastic models discussed

here for PMMA have been incorporated in both a characteristic code [60] and a finite-difference code [61]. Another aspect yet to be studied in depth is the extension to other geometrical configurations to include two- and three-dimensional effects. In this regard, Nunziato, Schuler and Walsh [50] have considered the bulk response of nonlinear materials and proposed a method for determining the material functions which govern this response. Furthermore, Yuan and Lianis [62] have considered wave propagation in nonlinear viscoelastic rods with the aim of determining the relevant material functions from a series of wave propagation experiments. In both of these studies the constitutive equation of finite linear viscoelasticity [4] is employed and thermodynamic influences are neglected.

Acknowledgments—We would like to express our thanks to W. Herrmann, who encouraged the preparation of this article; to M. E. Gurtin for his valuable suggestions with regard to the presentation; and to L. W. Davison, S. W. Key, D. E. Munson and H. J. Sutherland for their critical comments on a previous draft of this article. We would also like to thank Mrs. A. Hostetter for her assistance in the preparation of the manuscript.

Finally, we would like to express our appreciation to many of our colleagues in the field of wave propagation for the valuable and stimulating discussions which we had during the course of our investigations.

This work was supported by the United States Atomic Energy Commission.

REFERENCES

[1] C. Truesdell and R. A. Toupin, The classical field theories. *Handbuch der Physik*, III/1, edited by S. Flügge. Springer (1960).
[2] B. D. Coleman and M. E. Gurtin, Waves in materials with memory II. On the growth and decay of one-dimensional acceleration waves. *Arch. Ration. Mech. Analysis* **19**, 239 (1965).
[3] B. D. Coleman and W. Noll, An approximation theorem for functionals with applications in continuum mechanics. *Arch. Ration. Mech. Analysis* **6**, 355 (1960).
[4] B. D. Coleman and W. Noll, Foundations of linear viscoelasticity. *Rev. Mod. Phys.* **33**, 239 (1961). Erratum *ibid.* **36**, 1103 (1964).
[5] B. D. Coleman, M. E. Gurtin and I. Herrera, Waves in materials with memory I. The velocity of one-dimensional shock and acceleration waves. *Arch. Ration. Mech. Analysis* **19**, 1 (1965).
[6] R. M. Bowen and P. J. Chen, Thermodynamic restriction on the initial slope of the stress-relaxation function. *Arch. Ration. Mech. Analysis*, forthcoming.
[7] M. E. Gurtin and I. Herrera, On dissipation inequalities and linear viscoelasticity. *Quart. appl. Math.* **23**, 235 (1965).
[8] P. Bailey and P. J. Chen, On the local and global behavior of acceleration waves. *Arch. Ration. Mech. Analysis* **41**, 121 (1971). Addendum: Asymptotic behavior. *ibid.* **44**, 212 (1972).
[9] E. Varley, Acceleration fronts in viscoelastic materials. *Arch. Ration. Mech. Analysis* **19**, 215 (1965).
[10] B. D. Coleman, J. M. Greenberg and M. E. Gurtin, Waves in materials with memory V. On the amplitude of acceleration waves and mild discontinuities. *Arch. Ration. Mech. Analysis* **22**, 333 (1966).
[11] W. Noll, On the continuity of the solid and fluid states, *J. Ration. Mech. Analysis* **4**, 3 (1955).
[12] E. K. Walsh and K. W. Schuler, Acceleration wave propagation in a nonlinear viscoelastic solid. *J. appl. Mech.* to be published.
[13] P. J. Chen and M. E. Gurtin, On the growth of one-dimensional shock waves in materials with memory. *Arch. Ration. Mech. Analysis* **36**, 33 (1970).
[14] R. R. Huilgol, Growth of plane shock waves in materials with memory. *Int. J. Engng. Sci.* **11**, 75 (1973).
[15] J. Lubliner and G. A. Secor, The Propagation of Shock Waves in Nonlinear Viscoelastic Materials. Structural Engineering Laboratory Rept. 66-11, Univ. Calif. Berkeley (1966).
[16] G. E. Duvall and R. C. Alverson, Fundamental Research in Support of Vela-Uniform. Tech. Summary Rept. 4, Stanford Research Institute, Menlo Park (1963).
[17] T. J. Ahrens and G. E. Duvall, Stress relaxation behind elastic shock waves in rocks. *J. Geophys. Res.* **71**, 4349 (1966).
[18] E. H. Lee and I. Kanter, Wave propagation in finite rods of viscoelastic material. *J. appl. Phys.* **24**, 1115 (1953).
[19] B. T. Chu, Stress Waves in Isotropic Viscoelastic Materials. Division of Engineering Rept., Brown University, Providence (1962).

[20] K. C. VALANIS, Propagation and attenuation of waves in linear viscoelastic solids. *J. Math. Phys.* **44**, 227 (1965).
[21] A. C. PIPKIN, Shock structure in a viscoelastic fluid. *Quart. appl. Math.* **23**, 297 (1966).
[22] J. M. GREENBERG, The existence of steady shock waves in nonlinear materials with memory. *Arch. Ration. Mech. Analysis* **24**, 1 (1967).
[23] J. M. GREENBERG, Existence of steady waves for a class of nonlinear dissipative materials. *Quart. appl. Math.* **26**, 27 (1968).
[24] L. M. BARKER and R. E. HOLLENBACH, Shock wave studies of PMMA, fused silica and sapphire. *J. appl. Phys.* **41**, 4208 (1970).
[25] K. W. SCHULER, Propagation of steady shock waves in polymethyl methacrylate. *J. Mech. Phys. Solids* **18**, 277 (1970).
[26] L. M. BARKER and R. E. HOLLENBACH, System for measuring the dynamic properties of materials. *Rev. Sci. Inst.* **35**, 742 (1964).
[27] L. M. BARKER and R. E. HOLLENBACH, Interferometer technique for measuring the dynamic mechanical properties of materials. *Rev. Sci. Inst.* **36**, 1617 (1965).
[28] L. M. BARKER, The fine structure of compressive and release wave shapes in aluminum measured by the velocity interferometer technique. *Behavior of Dense Media Under High Dynamic Pressures*. p. 483. Gordon and Breach (1968).
[29] J. R. ASAY, D. L. LAMBERSON and A. H. GUENTHER, Pressure and temperature dependence of the acoustic velocities in polymethyl methacrylate. *J. appl. Phys.* **40**, 1768 (1969).
[30] J. W. NUNZIATO and H. J. SUTHERLAND, Acoustical determination of stress relaxation functions for polymers. *J. appl. Phys.* **44**, 184 (1973).
[31] W. HERRMANN and J. W. NUNZIATO, Nonlinear constitutive equations. *Dynamic Behavior of Materials Under Impulsive Loading*, edited by P. C. CHOU. forthcoming.
[32] K. W. SCHULER, The speed of release waves in polymethyl methacrylate. *Proc. of the 5th Symposium on Detonation*. U.S. Government Printing Office (1970).
[33] K. W. SCHULER and J. W. NUNZIATO, The dynamic mechanical behavior of polymethyl methacrylate. *Rheologica Acta*. forthcoming.
[34] K. W. SCHULER and E. K. WALSH, Critical-induced acceleration for shock propagation in polymethyl methacrylate. *J. appl. Mech.* **38**, 641 (1971).
[35] P. J. CHEN, M. E. GURTIN and E. K. WALSH, Shock amplitude variation in polymethyl methacrylate for fixed values of the strain gradient. *J. appl. Phys.* **41**, 3557 (1970).
[36] J. W. NUNZIATO and K. W. SCHULER, Shock pulse attenuation in a nonlinear viscoelastic solid. *J. Mech. Phys. Solids* to be published.
[37] L. D. BERTHOLF and M. L. OLIVER, Approximate Analytic Expressions for the Attenuation of a Triangular Pressure Pulse with Distance. Sandia Laboratories Rept. RR-69-596, Albuquerque (1970).
[38] G. R. FOWLES, Attenuation of the shock wave produced in a solid by a flying plate. *J. appl. Phys.* **31**, 655 (1960).
[39] P. J. CHEN and M. E. GURTIN, On the use of experimental results concerning steady shock waves to predict the acceleration wave response of nonlinear viscoelastic materials. *J. appl. Mech.* **39**, 295 (1972).
[40] T. Y. THOMAS, The growth and decay of sonic discontinuities in ideal gases. *J. Math. Mech.* **6**, 455 (1957).
[41] B. D. COLEMAN and M. E. GURTIN, Waves in materials with memory III. Thermodynamic influences on the growth and decay of acceleration waves. *Arch. Ration. Mech. Analysis* **19**, 266 (1965).
[42] W. A. DAY, *The Thermodynamics of Simple Materials with Fading Memory*. Springer (1972).
[43] B. D. COLEMAN, Thermodynamics of materials with memory. *Arch. Ration. Mech. Analysis* **17**, 1 (1964).
[44] V. J. MIZEL and C. C. WANG, A fading memory hypothesis which suffices for chain rules. *Arch. Ration. Mech. Analysis* **28**, 124 (1966).
[45] B. D. COLEMAN, Thermodynamics, strain impulses and viscoelasticity. *Arch. Ration. Mech. Analysis* **17**, 230 (1964).
[46] B. D. COLEMAN and M. E. GURTIN, Waves in materials with memory IV. Thermodynamics and the velocity of general acceleration waves. *Arch. Ration. Mech. Analysis* **19**, 317 (1965).
[47] J. W. NUNZIATO and E. K. WALSH, Propagation of steady shock waves in nonlinear thermoviscoelastic solids. *J. Mech. Phys. Solids* to be published.
[48] J. W. NUNZIATO and E. K. WALSH, Instantaneous and equilibrium Grüneisen parameters for a nonlinear viscoelastic polymer. *J. appl. Phys.* **44**, 1207 (1973).
[49] J. W. NUNZIATO and W. HERRMANN, The general theory of shock waves in elastic nonconductors. *Arch. Ration. Mech. Analysis* **47**, 272 (1972).
[50] J. W. NUNZIATO, K. W. SCHULER and E. K. WALSH, The bulk response of viscoelastic solids. *Trans. Soc. Rheol.* **16**, 15 (1972).
[51] J. G. CURRO, Hydrostatic equations of state for polymers. *J. Macro. Sci. Rev. in Macro. Chem.* forthcoming.
[52] Y. S. TOULOUKIAN, *Thermophysical properties of high temperature solid materials*, Vol. 5, Part II. Macmillan (1967).

[53] P. HEYDEMANN and H. D. GUICKING, Specific volume of polymers as a function of temperature and pressure. *Koll. Zeit.-Zeit. für Poly.* **193**, 16 (1963).
[54] B. D. COLEMAN and M. E. GURTIN, Thermodynamics and one-dimensional shock waves in materials with memory. *Proc. R. Soc.* **A, 292**, 562 (1966).
[55] P. J. CHEN and M. E. GURTIN, Thermodynamic influences on the growth of one-dimensional shock waves in materials with memory. *Z. Angew. Math. Phys.* **23**, 69 (1972).
[56] J. D. ACHENBACH, S. M. VOGEL and G. HERRMANN, On stress waves in viscoelastic media conducting heat. *Irreversible Aspects of Continuum Mechanics and Transfer of Physical Characteristics in Moving Fluids*, edited by H. PARKUS and L. I. SEDOV. Springer (1968).
[57] J. D. ACHENBACH and G. HERRMANN, Propagation of second-order thermomechanical disturbances in viscoelastic solids. *Thermoinelasticity*, edited by B. A. BOLEY, Springer (1970).
[58] J. DUNWOODY, One-dimensional shock waves in heat conducting materials with memory. 1. Thermodynamics. *Arch. Ration. Mech. Analysis* **47**, 117 (1972).
[59] J. W. NUNZIATO and E. K. WALSH, Amplitude behavior of shock waves in a thermoviscoelastic solid. *Int. J. Solids Structures* to be published.
[60] D. L. HICKS and D. B. HOLDRIDGE, The CONCHAS Wavecode. Sandia Laboratories Rept. RR-72-0451, Albuquerque (1972).
[61] R. J. LAWRENCE, A General Viscoelastic Constitutive Relation for Use in Wave Propagation Calculations. Sandia Laboratories Rept. RR-72-0114, Albuquerque (1972).
[62] H. L. YUAN and G. LIANIS, Experimental investigation of wave propagation in nonlinear viscoelastic materials. *Rheological Acta* to be published.

(*Received* 5 *February* 1973)

Абстракт—В работе дается обзор некоторых последных, теоретических и экспериментальных разработок в области распространения нелинейных, вязкоупругих волн. Ограничивая внимание к случаю одноразмерной деформации, пересматриваются теории распространения ударных и ускоренных волн в общих материалах с памятью. Обсуждается, также, корреляция между этими теоретическими предсказаниями и некоторыми последными экспериментальными результатами, полученными для определенных твердых тел из полимеров. Основным для этой работы является существование стационарных ударных волн и факт, что можно эти волны образовывать экспериментально для одноразмерного очертания. На основе экспериментальных наблюдений такихже стационарных волн, дается очерк методики определения функций поведения материалов, необходимых для предсказания роста и затухания ударных и ускоренных волн в вязкоупругих материалах. Кроме того указано, что на основе применения особого, конститутивного предположения (либо вполне механического либо термодинамического) можно определить полное одно размерное конститутивное уравнение поведения материала, как ряз из измерений стационарной ударной волны.